Novel Endocranial Data on the Early Therocephalian *Lycosuchus vanderrieti* Underpin High Character Variability in Early Theriodont Evolution

Luisa C. Pusch [1,2]*, Jasper Ponstein [1,2], Christian F. Kammerer [3,4] and Jörg Fröbisch [1,2,4]

[1] Museum für Naturkunde, Leibniz-Institut für Evolutions- und Biodiversitätsforschung, Berlin, Germany, [2] Institut für Biologie, Humboldt-Universität zu Berlin, Berlin, Germany, [3] North Carolina Museum of Natural Sciences, Raleigh, NC, United States, [4] Evolutionary Studies Institute, University of the Witwatersrand, Johannesburg, South Africa

Therocephalia is one of the major therapsid clades and ranges from the middle Permian to Middle Triassic. The earliest therocephalians were large-bodied predators whose fossils are common in middle Permian rocks of South Africa, but have received little study. Here we present a redescription of the skull of the early therocephalian *Lycosuchus* based on a specimen from the middle Permian *Tapinocephalus* Assemblage Zone of the South African Karoo Basin. By using a computed tomographic (CT) reconstruction of this specimen, we describe for the first time several endocranial characters of this taxon including a highly ramified maxillary canal and the inner ear, which is characterized by a lengthened lateral semicircular canal, a feature previously only known from the anomodont *Kawingasaurus* among non-mammalian therapsids, and the presence of a cochlear recess, so far only known within Therocephalia from the highly specialized Triassic taxon *Microgomphodon*. We also provide new insights into patterns of tooth replacement in lycosuchids, which have proven controversial for this taxon. Craniodental characters generally support the placement of *Lycosuchus* as the most basal taxon in therocephalian phylogeny. The morphology of the maxillary canal and inner ear reveal a mosaic of features indicating a complex history of character acquisition and loss in Therocephalia, comparable to that of cynodonts.

Keywords: therapsida, computed tomography, endocranial anatomy, maxillary canal, bony labyrinth, mosaic evolution, mandible

INTRODUCTION

The advent of widely-used computed tomographic (CT) imaging on fossil specimens has allowed paleontologists unprecedented access to the once-obscure internal features of vertebrate crania. In the context of mammalian origins, these novel endocranial data have been instrumental in elucidating patterns of brain and ear evolution, facial innervation, and the evolution of endothermy in non-mammalian therapsids (e.g., Rodrigues et al., 2013, 2014; Crompton et al., 2015, 2017; Laaß, 2015a,b, 2016; Benoit et al., 2016a,b, 2017a,b,c, 2018, 2019; Araújo et al., 2017, 2018; Bendel et al., 2018; Pusch et al., 2019). As the therapsid clade ancestral to (and including) modern

mammals, Cynodontia has been the primary focus for CT-assisted morphological studies in Synapsida (e.g., Rowe et al., 1993; Rodrigues et al., 2013, 2014; Crompton et al., 2015, 2017; Benoit et al., 2016a, 2019; Pavanatto et al., 2019; Pusch et al., 2019). By contrast, Therocephalia, generally considered the sister-group of Cynodontia (e.g., Hopson and Barghusen, 1986; Hopson, 1991; Huttenlocker, 2009; Huttenlocker and Sidor, 2016; Huttenlocker and Smith, 2017; but see Abdala, 2007; Botha et al., 2007), has received little study.
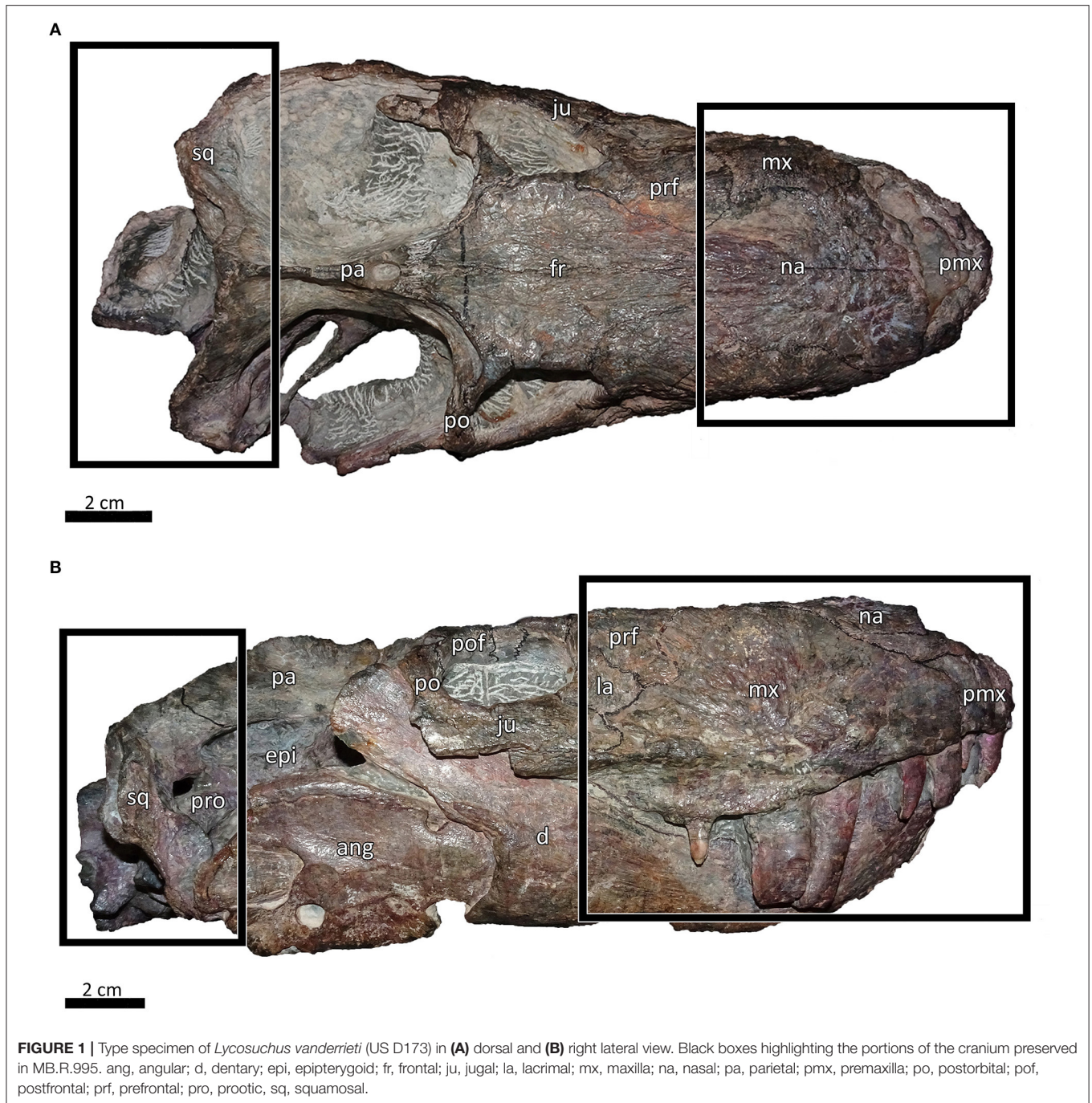
Therocephalia is a species-rich and ecomorphologically varied group ranging from the middle Permian to the Middle Triassic, with highest diversity in the late Permian (Abdala et al., 2008; Huttenlocker et al., 2011; Huttenlocker, 2014; Huttenlocker and Smith, 2017). The earliest known representatives of this group have been reported from the middle Permian *Eodicynodon* Assemblage Zone (AZ) in the Karoo Basin of South Africa (Abdala et al., 2008), and they are the most abundant group of predatory therapsids in the subsequent, middle–earliest late Permian *Tapinocephalus* and *Pristerognathus* AZs, with hundreds of known specimens (Smith et al., 2012). Despite their abundance, these early therocephalian taxa have received little study relative to their later Permo-Triassic relatives. Two families of early therocephalians are current recognized (Scylacosauridae and Lycosuchidae), both consisting of large-bodied (1–3 m body length) predators (van den Heever, 1994; Abdala et al., 2014a). Scylacosaurids exhibit long, comparably narrow snouts and include the oldest known therocephalians (both taxa reported from the *Eodicynodon* AZ are scylacosaurids; Abdala et al., 2008). By contrast, lycosuchids are characterized by relatively short, broad snouts and reduction of the postcanine dentition (van den Heever, 1994; Abdala et al., 2008, 2014a).

Abdala et al. (2014a) recently described new lycosuchid specimens and reviewed the family's taxonomy, recognizing only two valid species: *Lycosuchus vanderrieti* and *Simorhinella baini*. *Simorhinella* is restricted to the *Tapinocephalus* AZ, whereas *Lycosuchus* ranges from the uppermost *Tapinocephalus* AZ through the *Pristerognathus* AZ. Cladistic analyses have found that *Lycosuchus* occupies the most basal position in therocephalian phylogeny (e.g., van den Heever, 1994; Abdala, 2007; Botha et al., 2007; Huttenlocker, 2009; Huttenlocker et al., 2011; Huttenlocker and Sidor, 2016; Huttenlocker and Smith, 2017; Kammerer and Masyutin, 2018). The position of *Simorhinella* is less certain, and it has generally been excluded from phylogenetic analyses of Therocephalia. Abdala et al. (2014a) noted that *Simorhinella* shares some features with scylacosaurids to the exclusion of *Lycosuchus* (e.g., presence of a median vomerine crest, ventral extension of ridges from the transverse processes of the pterygoid), suggesting that Lycosuchidae may be paraphyletic. More recently, Liu and Abdala (2019) recovered *Gorynychus masyutinae*, a Russian taxon originally found to be the sister-taxon of Eutherocephalia (Kammerer and Masyutin, 2018), as the sister taxon of *Lycosuchus*. These variable results indicate substantial instability in basal (i.e., non-eutherocephalian) therocephalian phylogeny, probably associated with extensive homoplasy in this group (Kammerer and Masyutin, 2018) and necessitating a more detailed understanding of the anatomy of basal therocephalians.

Although the holotype of *Lycosuchus vanderrieti* consists of a complete, well-preserved skull and jaws (US D173, **Figure 1**), only superficial accounts of its anatomy have been published in the literature. Broom (1903) initially described the taxon, but discussed its anatomy only briefly. Boonstra (1964) described additional lycosuchid specimens, but primarily dealt with their postcranial anatomy. Not until the work of van den Heever (1980, 1987, 1994) was there extensive description of cranial morphology in the group. Because van den Heever (1994) based his description on semi-disarticulated lycosuchid crania (CGS C60 and CGS M793), he was even able to discuss portions of the anatomy rarely visible in therocephalian specimens (e.g., the medial surface of the snout wall). Nevertheless, he was unable to address many aspects of the endocranial anatomy in *Lycosuchus* due to technological limitations of the time (and rarity of the study taxon making serial sectioning inadvisable).

Olson (1944) first described internal skull anatomy in several purported basal therocephalians based on serial sections, but more recent research has demonstrated that some of these specimens instead represent gorgonopsians (van den Heever and Hopson, 1982). Hillenius (1994) described ridges on the internal ventral margin of the nasal bones in the basal therocephalian *Glanosuchus*, which he argued supported maxilloturbinals, though this has been disputed (Sigurdsen, 2006). Sigurdsen (2006) provided the first detailed description of many therocephalian endocranial characters on the basis of serial sections of an indeterminate akidnognathid. More recent, CT-based investigations by Sigurdsen et al. (2012) and Benoit et al. (2016a,b, 2017a,b) have shed additional light on therocephalian endocranial anatomy, providing new information on facial innervation and brain and inner ear morphology. Among this new data, Benoit et al. (2017b) presented the first instance of a cochlear recess in the inner ear of a therocephalian, in the highly specialized Triassic taxon *Microgomphodon*.

Here, we present new information on the skull of *Lycosuchus vanderrieti* based on MB.R.995 from the *Tapinocephalus* AZ, which consists of a partial snout, braincase and mandible. This specimen was initially described by Janensch (1952), but his description focused only on surface details of the lower jaw. By using a computed tomographic (CT) reconstruction of this specimen, we describe for the first time several endocranial characters of this taxon and also provide new insights into patterns of tooth replacement in lycosuchids, which have historically been controversial (Broom, 1903; Boonstra, 1969; van den Heever, 1980). MB.R.995 includes a complete, well-preserved lower jaw, an element rarely discussed in previous accounts of lycosuchid anatomy (van den Heever, 1994 provided a thorough generalized description of the jaw in early therocephalians, but not *Lycosuchus* specifically). Although the jaw of MB.R.995 has been discussed in the literature before, the brief description by Janensch (1952) provided little information beyond the shape of the reflected lamina of the angular. Our redescription of this element provides substantial new data on its anatomy and permits broader comparisons with other therocephalians. CT-reconstruction of the jaw and cranium of *Lycosuchus* allows us

FIGURE 1 | Type specimen of *Lycosuchus vanderrieti* (US D173) in **(A)** dorsal and **(B)** right lateral view. Black boxes highlighting the portions of the cranium preserved in MB.R.995. ang, angular; d, dentary; epi, epipterygoid; fr, frontal; ju, jugal; la, lacrimal; mx, maxilla; na, nasal; pa, parietal; pmx, premaxilla; po, postorbital; pof, postfrontal; prf, prefrontal; pro, prootic, sq, squamosal.

to evaluate the character support for *Lycosuchus* as the most basal taxon in therocephalian phylogeny and discuss character evolution in Therocephalia.

MATERIALS AND METHODS

The incomplete cranium and associated mandible of the specimen of *Lycosuchus vanderrieti* described herein (MB.R.995,

Figures 2–4, 10, 12) are part of the collection of the Museum für Naturkunde Berlin. This specimen was collected by W. Janensch in the *Tapinocephalus* AZ of Letjesbosch near Beaufort West, South Africa in 1929, and later prepared by E. Siegert and J. Schrober (Janensch, 1952). Although fragmented, the existing parts of the skull of MB.R.995 are in relatively good condition. The bones forming the snout and parts of the palate are preserved up to the level of the pterygoid, of which only the anterior part is preserved. The total length of the partial snout is ∼19.5 cm and
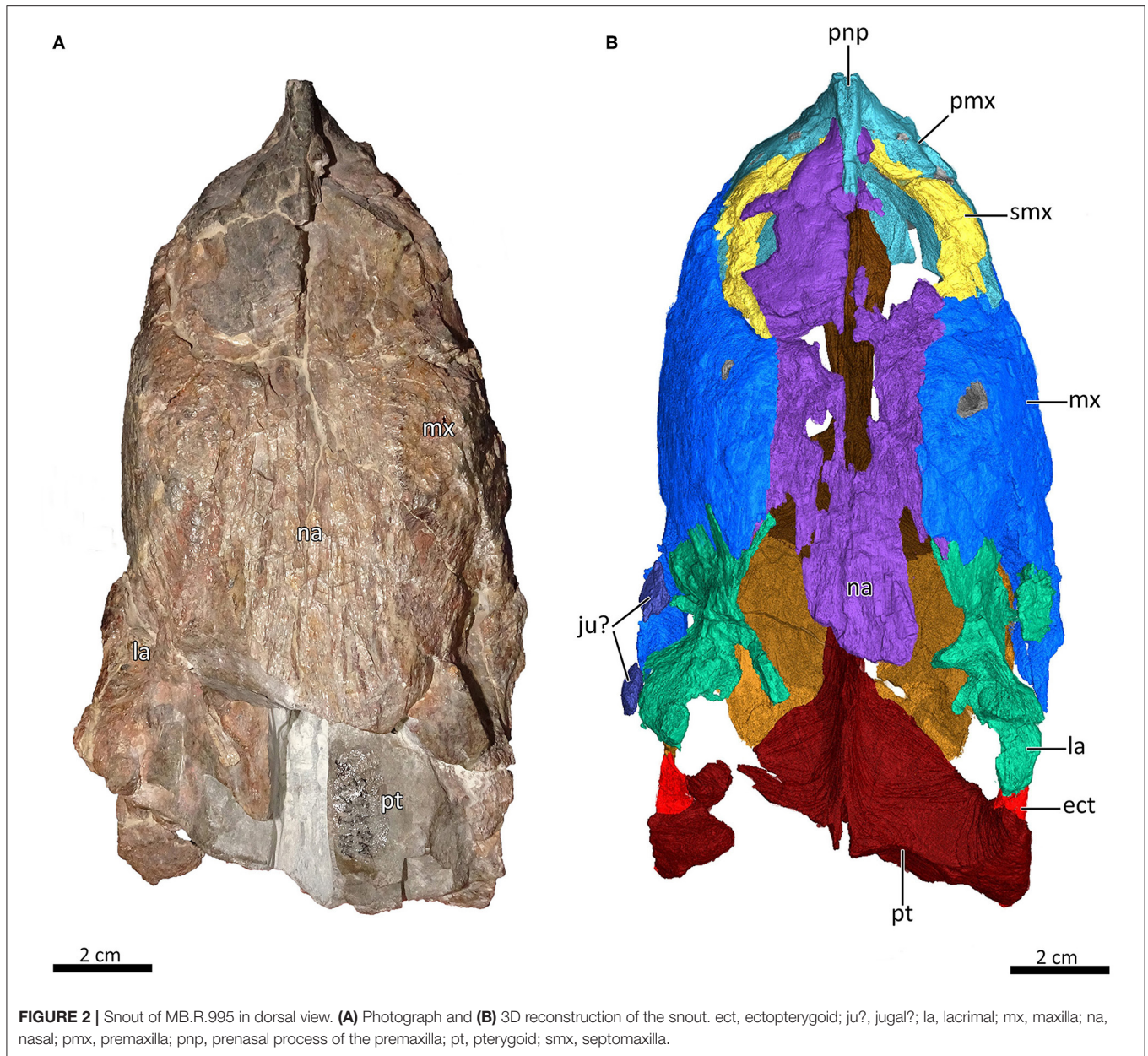
FIGURE 2 | Snout of MB.R.995 in dorsal view. **(A)** Photograph and **(B)** 3D reconstruction of the snout. ect, ectopterygoid; ju?, jugal?; la, lacrimal; mx, maxilla; na, nasal; pmx, premaxilla; pnp, prenasal process of the premaxilla; pt, pterygoid; smx, septomaxilla.
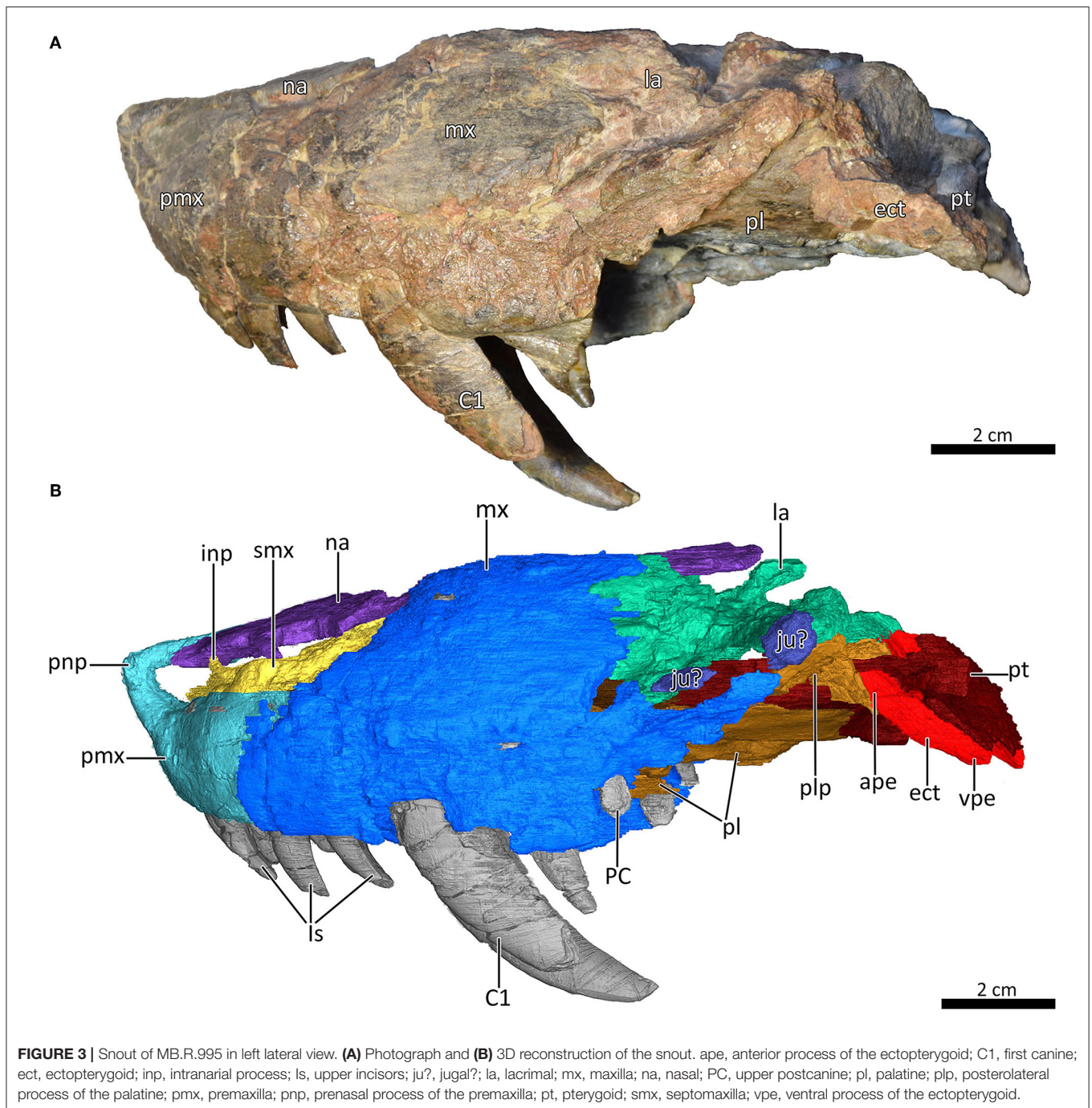
its maximum width is 9.4 cm. The partially preserved braincase primarily consists of bones forming the occiput and is about 7.9 cm high and 12 cm wide. Both lower jaw rami are preserved, but the left one is more complete, with the postdentary bones missing on the right. We scanned only the left mandibular ramus, which is ∼21.5 cm long.

MB.R.995 was CT scanned in the CT-Laboratory of the Museum für Naturkunde Berlin using an YXLON FF35 X-ray CT scanner. The complete scan sets consist of 3,154 (for the snout), 3,147 (for the braincase), and 2,354 (for the left mandible) slices. The slices were generated in coronal planes with a voxel size of 0.0486 mm (for the snout), 0.0366 mm (for the braincase), and 0.0323 mm (for the left mandible). Tube voltage ranged from 130 to 200 kV, and tube current from 40 to 172 μA. The visualization of the slices, virtual 3D rendering, and segmentation

of selected structures were performed using VGStudio Max 3.2 (Volume Graphics GmbH, Heidelberg, Germany) in the 3D Visualization Laboratory at the Museum für Naturkunde Berlin. The inner ear endocast was segmented from the sediment infilling the right bony labyrinth of the skull. Its measurements were taken using VGStudio Max and follow the protocol of Benoit et al. (2017b, **Figure 2**).

INSTITUTIONAL ABBREVIATIONS

CGS, Council for Geosciences, Pretoria, South Africa; MB.R., Museum für Naturkunde, Fossil Reptile Collection, Berlin, Germany; US, University of Stellenbosch, Stellenbosch, South Africa.

FIGURE 3 | Snout of MB.R.995 in left lateral view. **(A)** Photograph and **(B)** 3D reconstruction of the snout. ape, anterior process of the ectopterygoid; C1, first canine; ect, ectopterygoid; inp, intranarial process; ls, upper incisors; ju?, jugal?; la, lacrimal; mx, maxilla; na, nasal; PC, upper postcanine; pl, palatine; plp, posterolateral process of the palatine; pmx, premaxilla; pnp, prenasal process of the premaxilla; pt, pterygoid; smx, septomaxilla; vpe, ventral process of the ectopterygoid.
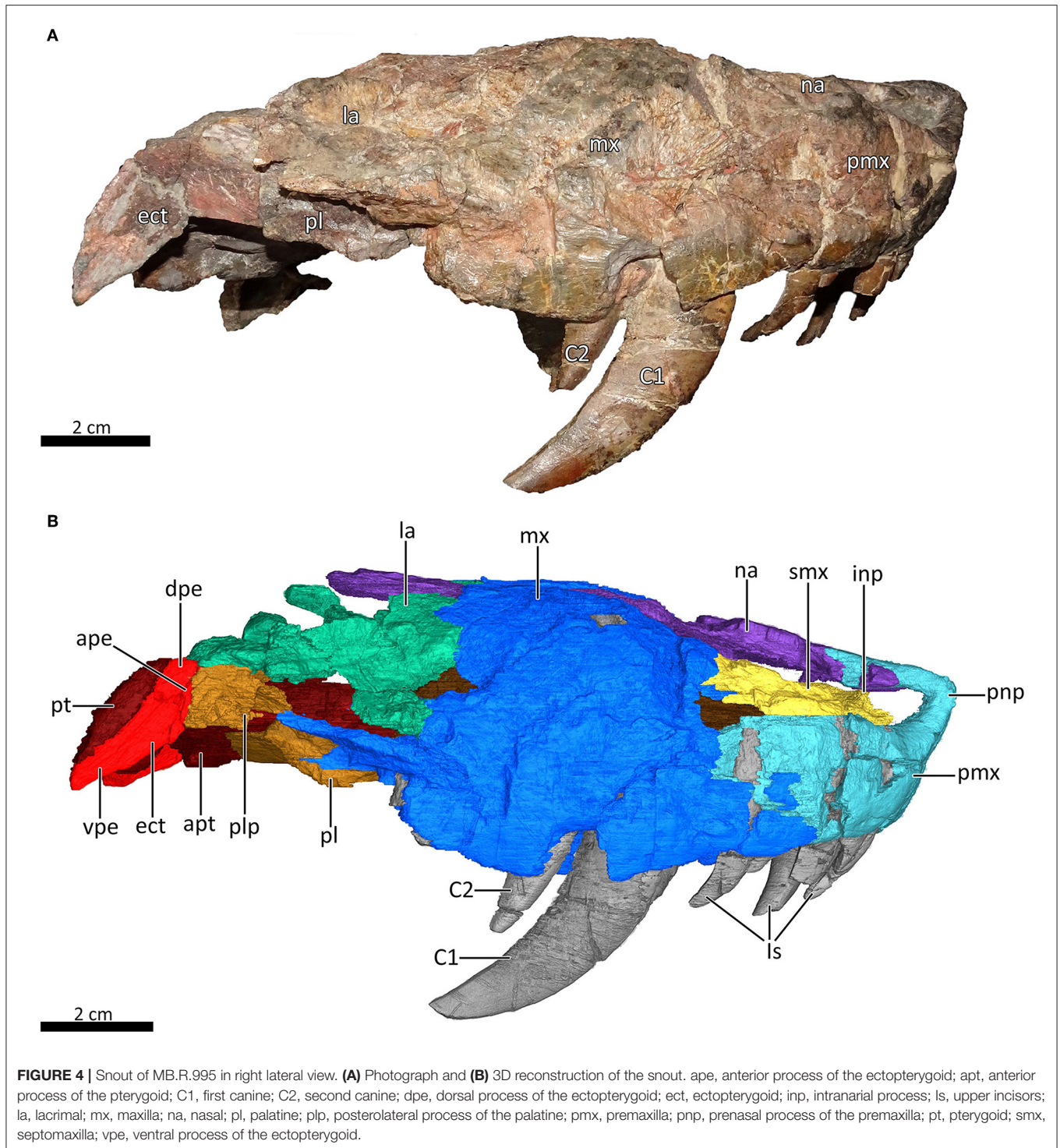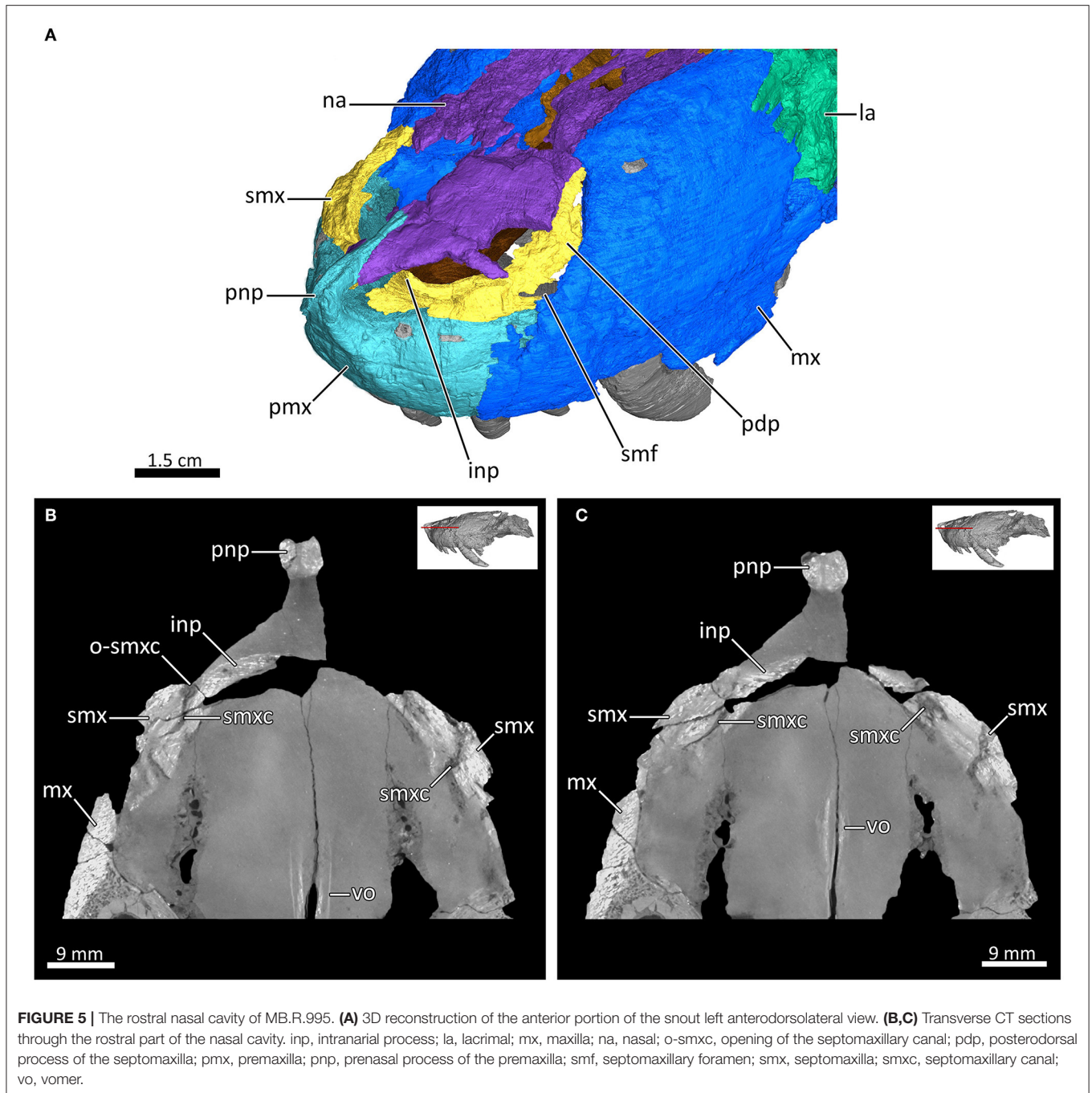
RESULTS

General Preservation

The left side of the snout of MB.R.995 is generally better preserved than the right one, with only the posterior portion of the snout better preserved on the right side. The portion of the palate consisting of the vomer and the palatine is well-prepared and its bone surface is in relatively good condition. The nasals are badly damaged, with the anterior portion of the right nasal bone almost completely missing. Both lacrimals are badly crushed, with only the anteromedial portions being relatively well-preserved (**Figures 2–4**, **5A**, **7**, **8**, **9A**). MB.R.995 is missing the prefrontals, frontals, postorbitals, postfrontals, zygomatic arches, most of the pterygoid and parabasisphenoid, the orbitosphenoid, epipterygoids, stapes, and the quadrate-quadratojugal complex. However, there seems to be at least a part of the posterior region of the parietal preserved in the damaged dorsal portion of the occiput. In addition, there are two small pieces of bone lateral to the left maxilla and lacrimal that may be parts of the jugal (**Figures 2–4**, **8**, **10**). Despite damage to the

FIGURE 4 | Snout of MB.R.995 in right lateral view. **(A)** Photograph and **(B)** 3D reconstruction of the snout. ape, anterior process of the ectopterygoid; apt, anterior process of the pterygoid; C1, first canine; C2, second canine; dpe, dorsal process of the ectopterygoid; ect, ectopterygoid; inp, intranarial process; ls, upper incisors; la, lacrimal; mx, maxilla; na, nasal; pl, palatine; plp, posterolateral process of the palatine; pmx, premaxilla; pnp, prenasal process of the premaxilla; pt, pterygoid; smx, septomaxilla; vpe, ventral process of the ectopterygoid.

dorsal and anterior portion of the braincase, the occiput is generally in relatively good condition, but preserves only part of the left squamosal, with the right squamosal absent entirely (**Figure 10**). The reader is therefore directed to the descriptions of Broom (1903) and van den Heever (1987, 1994) for additional information on the exterior morphology of these elements, based

on complete crania of *Lycosuchus*. The left mandible is long and fairly robust, as is typical of early therocephalians (van den Heever, 1987, 1994; Suchkova and Golubev, 2019). It is relatively well-preserved, with only the posterodorsal end of the coronoid process missing, broken above the dorsal margin of the surangular. However, enough of the coronoid process is

FIGURE 5 | The rostral nasal cavity of MB.R.995. **(A)** 3D reconstruction of the anterior portion of the snout left anterodorsolateral view. **(B,C)** Transverse CT sections through the rostral part of the nasal cavity. inp, intranarial process; la, lacrimal; mx, maxilla; na, nasal; o-smxc, opening of the septomaxillary canal; pdp, posterodorsal process of the septomaxilla; pmx, premaxilla; pnp, prenasal process of the premaxilla; smf, septomaxillary foramen; smx, septomaxilla; smxc, septomaxillary canal; vo, vomer.

preserved to show that it was free standing above the postdentary bones (**Figure 12**).

Snout

The premaxilla forms the anterior portion of the snout and is characterized by a tall, strongly arched prenasal (intranarial) process projecting beyond the anterior margin of main body of the premaxilla (**Figures 3**, **4**). The prenasal process continues posterodorsally as an elongate, narrow process extending between the nasals and the external naris

(**Figures 2–4**, **5A**, **7**, **8A**). This morphology is similar to that of the whaitsiid therocephalian *Theriognathus microps* (Huttenlocker and Abdala, 2015), although the posterior portion of the prenasal process of MB.R.995 is even longer than in *Theriognathus*. The facial surface of the premaxilla is broadly overlapped by the maxilla posteriorly, up to the level of I4 (**Figures 3B**, **4B**, **5A**, **8B**). Each premaxilla bears five incisors (damaged to varying degrees), which are enclosed in a broad ventral alveolar plate. The alveolus of the left I1 is almost completely empty, with only a fragment of the root present;

otherwise at least part of the crown is preserved for all other incisors (**Figures 3**, **4**, **7**, **8B**, **12**). Posteromedially, the premaxilla forms a short, posteriorly-located vomerine process, which underlies the anterior portion of the vomer (**Figures 7A,C**, **8**, **13D**). van den Heever (1987, 1994) questioned the presence of a vomerine process in *Lycosuchus,* because of the apparent absence of this feature in the specimen CGS M793. However, our results clearly show the presence of a vomerine process in MB.R.995, indicating that its absence in CGS M793 was a preservational artifact.
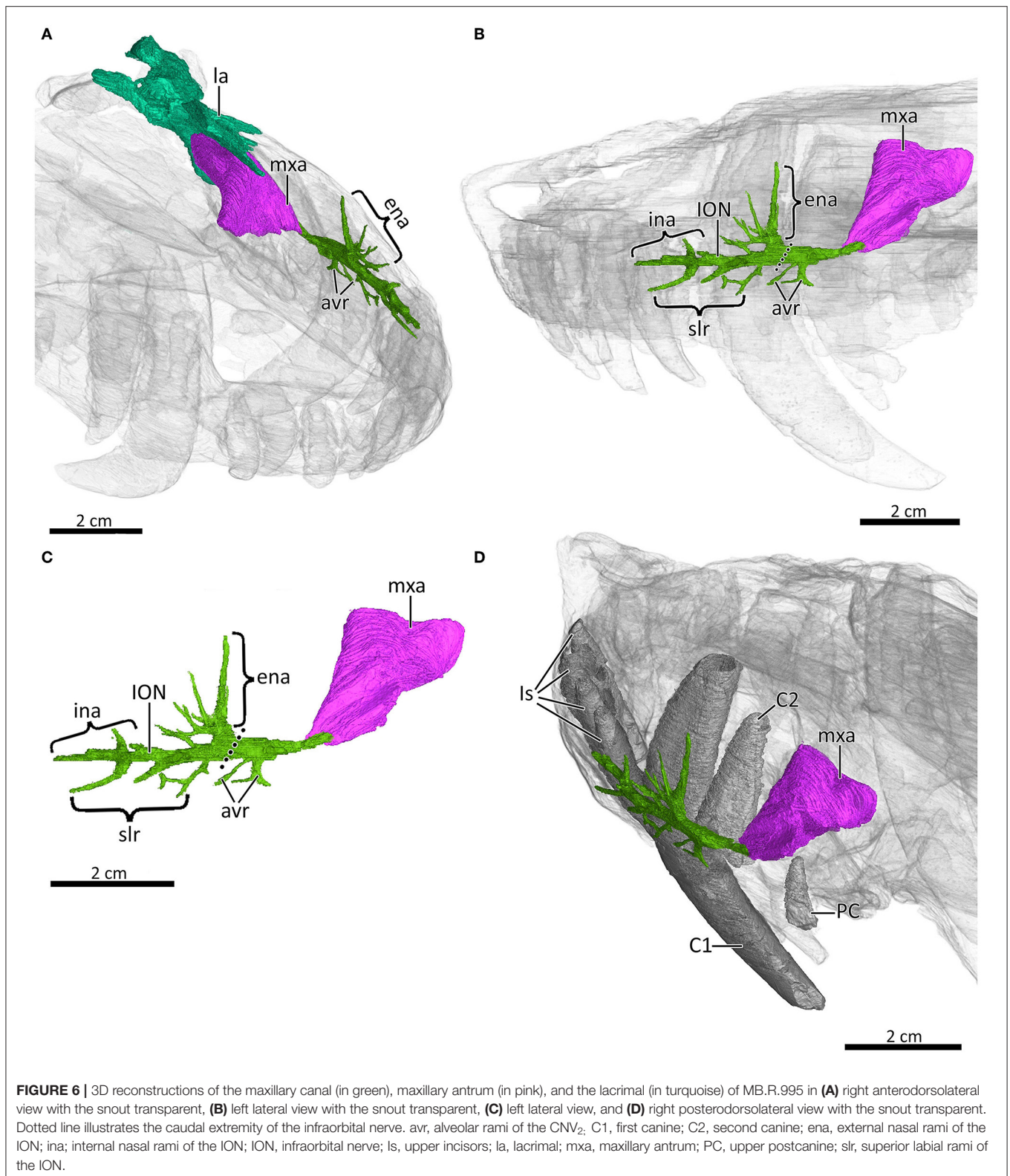
The septomaxilla is large and forms the posteroventral border of the external naris. Its footplate broadly contacts the premaxilla ventrally, making up the external narial floor (**Figures 2B**, **3B**, **4B**, **5**, **7**, **8A**). The anterior portion of the footplate curves inward, resting on a medial platform of the premaxilla. It bears a well-developed, transversely-oriented intranarial process (only preserved on the left side) (**Figures 3B**, **4B**, **5A**, **7A,B**). The dorsal tip of this process is just lateral to the anteriormost part of the nasal, nearly contacting it, though this extreme proximity is probably due to post mortem distortion, as it is broadly separated from the nasal in uncrushed skulls (see, e.g., van den Heever, 1994). The septomaxillary canal is clearly visible in section in the scan (**Figures 5B,C**). It enters the bone from the inside of the nasal cavity in the posterior region of the septomaxilla at the septomaxillary foramen. The latter is large and located on the lateral surface of the snout, bordered by the septomaxilla anteriorly and the maxilla posteriorly. The anterior opening of the septomaxillary canal is near the base of the intranarial process (**Figure 4**). Posterodorsal to the septomaxillary foramen, the septomaxilla has a facial (posterodorsal) process extending between the nasal and the maxilla (**Figures 2B**, **3B**, **4B**, **5A**, **7A,B**).

The nasal is a large bone forming the dorsal roof of the snout and the nasal cavity. Anteriorly, the nasal becomes wider and flatter in the region where it forms the dorsal margin of the external naris, but tapers at its anteriormost portion where it contacts the prenasal process of the premaxilla and nearly contacts the intranarial process of the left septomaxilla (**Figure 2**). The external naris appears unusually narrow in MB.R.995 (**Figures 3**, **4**, **5A**, **7A,B**) as a result of dorsoventral crushing in this specimen. Laterally, the nasal is overlapped by the dorsal lamina of the maxilla. Posterolaterally, the nasal would usually contact the prefrontal and the anterior margin of the frontal (missing in this specimen). In this area the posterior margin of the nasals, which is V-shaped in better preserved skulls of *Lycosuchus* (e.g., Broom, 1903; van den Heever, 1987, 1994), is also slightly crushed and incompletely preserved (**Figures 2B**, **3B**, **4B**, **5A**, **7A,B**). Internally, the ventral margin of the nasal is posteriorly overlain by the anterior process of the lacrimal, which is in turn overlapped by the maxilla (**Figures 7**, **9C**). Although badly damaged, the ventral surface of the nasal bones seems to be transversely concave, becoming flatter in the region where they usually contact the frontals and prefrontals. In this region, a pair of weakly preserved ridges occurs along the ventral surface of the nasal, parallel to the midline suture, which probably extended from the ventral surface of the frontals. These ridges probably would have stretched along the entire ventral surface

of the nasals, although this cannot be seen in this specimen due to damage (**Figure 9**). These ridges may have served as attachment points for cartilaginous nasal turbinals, as has been described for several therapsids in recent years (e.g., Kemp, 1979; Hillenius, 1994; Crompton et al., 2015, 2017; Bendel et al., 2018; Pusch et al., 2019). In therocephalians in particular, cartilaginous turbinals attaching to the nasals have been proposed for the basal taxon *Glanosuchus macrops* (Hillenius, 1994; van den Heever, 1994), akidnognathids (Sigurdsen, 2006), and for the baurioid *Tetracynodon darti* (Sigurdsen et al., 2012). A median ridge on the midline suture of the nasals, as has been inferred to support the dorsal edges of a cartilaginous internasal septum in cynodonts (Crompton et al., 2017), could not be observed. However, given the incompleteness of the nasals, its absence in *Lycosuchus* should not be taken as definite.

The maxilla is a large element, which forms most of the lateral surface of the snout and much of the side wall of the nasal cavity. It has a very high and broad facial lamina that largely excludes the nasal from sight in lateral view (which probably is not just an artifact of crushing, as the same is true in the relatively undistorted holotype, **Figure 1B**), and a posterolateral process that tapers gradually beneath the orbit, where it usually underlies the jugal. However, both maxillae are damaged in that area, and other than two possible fragments, the jugals are not preserved. Posteriorly and posterodorsally, the maxilla contacts the lacrimal (**Figures 2–4**, **8**). The external surface of the maxilla is finely rugose, especially in the dorsal region of the first canine where its root is exposed on the dorsal lamina of the maxilla. This rugosity is most clearly visible on the left maxilla, since the outer surface of the right maxilla is largely damaged. The internal surface of the facial portion of the maxilla is generally smooth and flat, but becomes substantially thicker anteriorly due to the large boss around the alveolus of the first canine. Immediately anterior to the canine boss and medioventral to the suture with the septomaxilla, the maxilla bears a small depression, the anterior maxillary fossa (**Figure 7**). This feature is also present in *Glanosuchus* (van den Heever, 1994) and the akidnognathid *Shiguaignathus wangi* (Liu and Abdala, 2017). By contrast, an anterior maxillary fossa is not known in the baurioid *Tetracynodon darti* (Sigurdsen et al., 2012). Posterior to the canine boss, there is a second depression, called the posterior maxillary fossa by van den Heever (1994) and the anterior maxillary sinus by Sigurdsen (2006). The anterior and posterior maxillary fossae seem to be simple artifacts of the extensive medial development of the canine boss. Along the majority of its ventral margin the maxilla contacts the palatine, starting anteromedial to the canine boss and ending posteriorly where the posterolateral process of the maxilla contacts the lateral margin of the posterolateral process of the palatine, which in turn contacts the anterior process of the ectopterygoid (**Figures 3B**, **4B**, **7**, **8**). However, due to damage to the maxilla, there is a small gap between it and the palatine here (**Figure 8**). According to van den Heever (1987, 1994), the posterolateral process of the maxilla overlies the lateral margin of the contact between the palatal process of the palatine and the anterior process of the ectopterygoid in that area.

FIGURE 6 | 3D reconstructions of the maxillary canal (in green), maxillary antrum (in pink), and the lacrimal (in turquoise) of MB.R.995 in (A) right anterodorsolateral view with the snout transparent, (B) left lateral view with the snout transparent, (C) left lateral view, and (D) right posterodorsolateral view with the snout transparent. Dotted line illustrates the caudal extremity of the infraorbital nerve. avr, alveolar rami of the CNV_2; C1, first canine; C2, second canine; ena, external nasal rami of the ION; ina; internal nasal rami of the ION; ION, infraorbital nerve; ls, upper incisors; la, lacrimal; mxa, maxillary antrum; PC, upper postcanine; slr, superior labial rami of the ION.
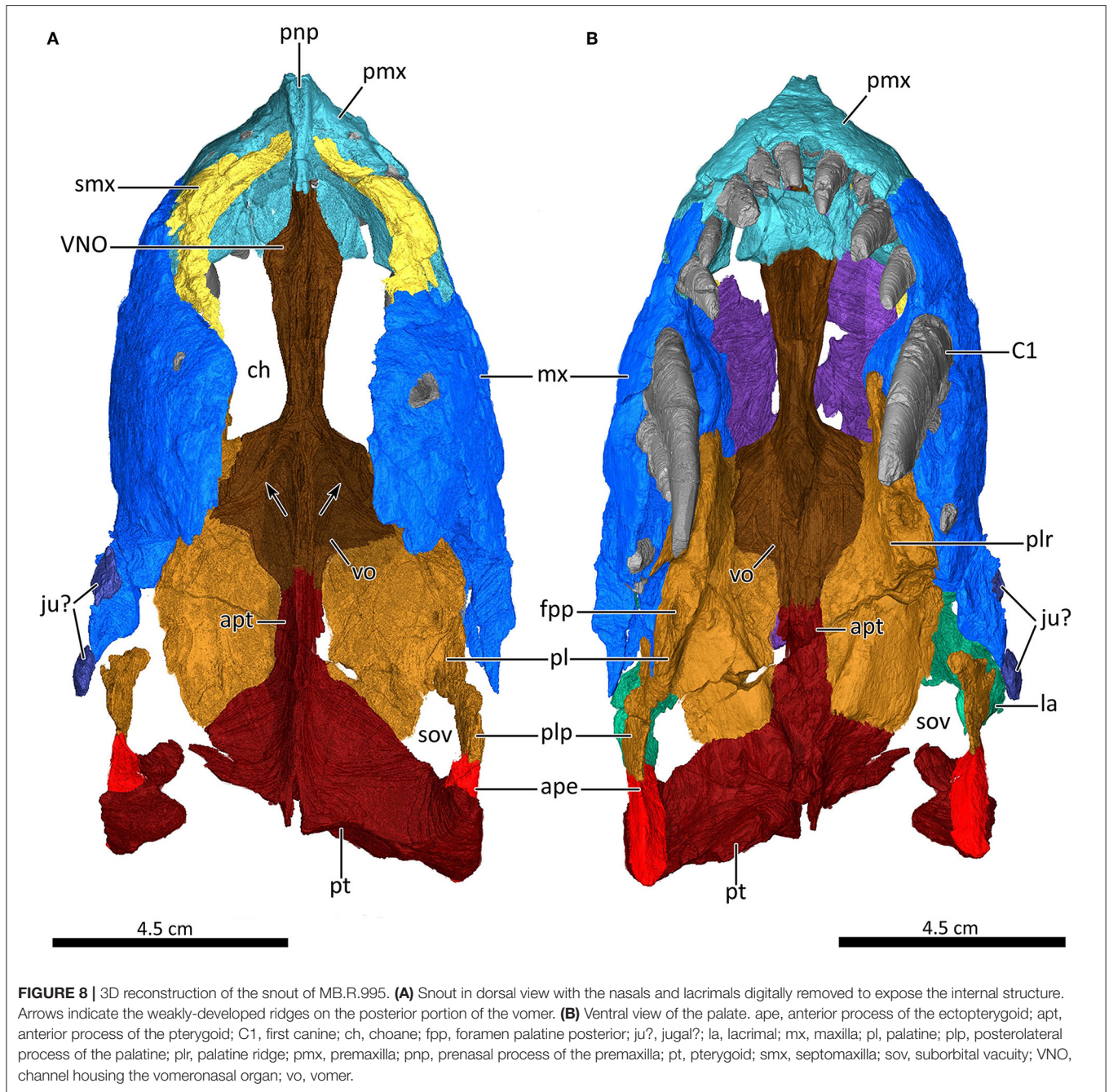
Posterior to the posterior maxillary fossa, in the region where the maxilla underlies the anterior margin of the lacrimal, the former appears slightly convex medially. A large, internal facial recess is present in this area of the maxilla, extending onto the medial surface of the anterior portion of the lacrimal (**Figures 6A**, **7**, **9C**, **13D**). This recess corresponds to the
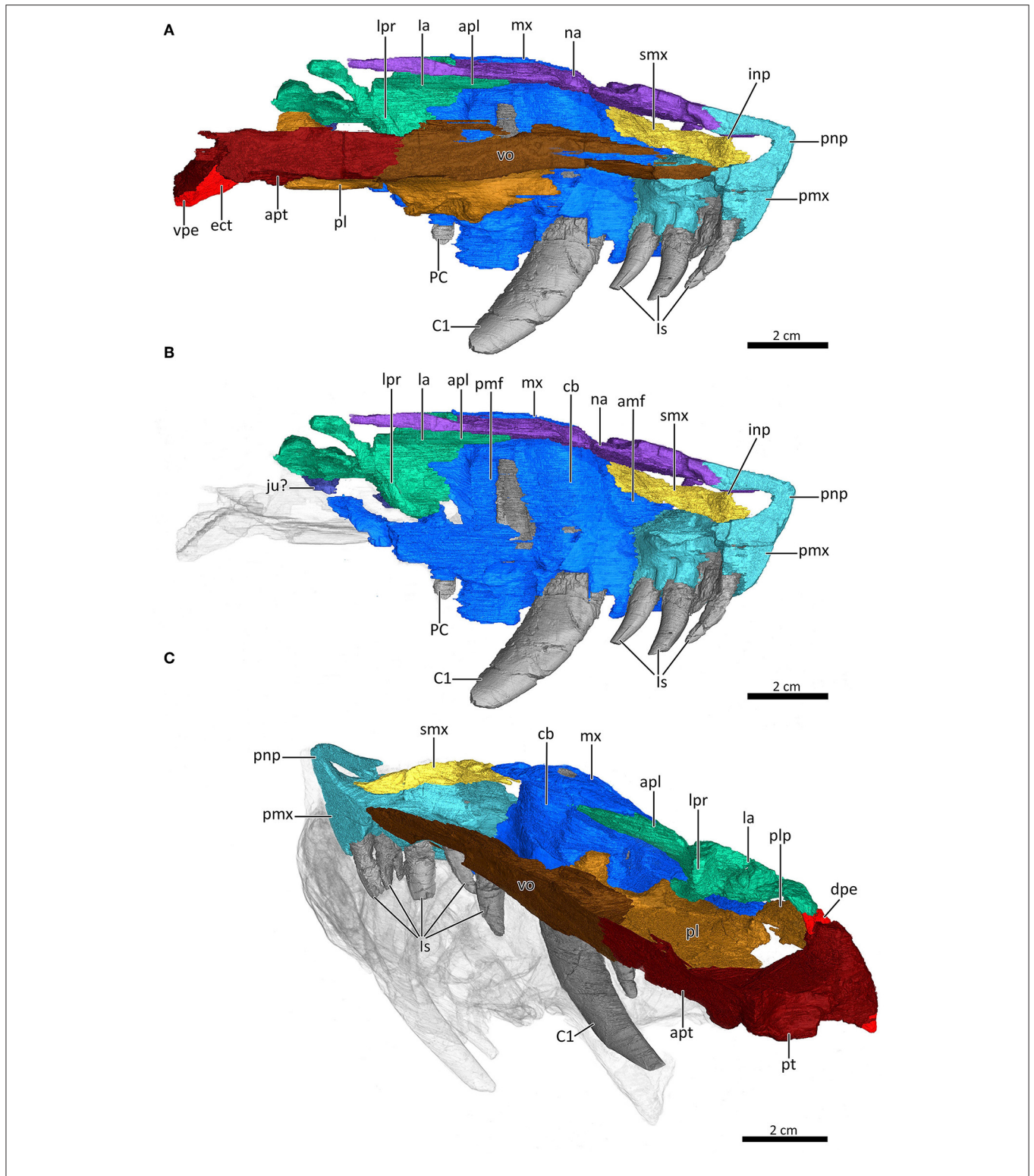
FIGURE 7 | Mid-sagittal section through the reconstructed snout of MB.R.995 to show its internal morphology. **(A,B)** Internal view of the left nasal region with the vomer, palatine, and ectopterygoid digitally removed in **(B)** to expose the internal structure. **(C)** Internal morphology of the right nasal region in posterodorsolateral view with the nasal digitally removed to expose the internal structure. amf, anterior maxillary fossa; apl, anterior process of the lacrimal; apt, anterior process of the pterygoid; C1, first canine; cb, canine boss; dpe, dorsal process of the ectopterygoid; ect, ectopterygoid; inp, intranarial process; ls, upper incisors; ju?, jugal?; la, lacrimal; lpr, lacrimo-palatine ridge; mx, maxilla; na, nasal; PC, upper postcanine; pl, palatine; plp, posterolateral process of the palatine; pmf, posterior maxillary fossa; pmx, premaxilla; pnp, prenasal process of the premaxilla; pt, pterygoid; smx, septomaxilla; vo, vomer; vpe, ventral process of the ectopterygoid.

FIGURE 8 | 3D reconstruction of the snout of MB.R.995. **(A)** Snout in dorsal view with the nasals and lacrimals digitally removed to expose the internal structure. Arrows indicate the weakly-developed ridges on the posterior portion of the vomer. **(B)** Ventral view of the palate. ape, anterior process of the ectopterygoid; apt, anterior process of the pterygoid; C1, first canine; ch, choane; fpp, foramen palatine posterior; ju?, jugal?; la, lacrimal; mx, maxilla; pl, palatine; plp, posterolateral process of the palatine; plr, palatine ridge; pmx, premaxilla; pnp, prenasal process of the premaxilla; pt, pterygoid; smx, septomaxilla; sov, suborbital vacuity; VNO, channel housing the vomeronasal organ; vo, vomer.

posterior maxillary sinus of van den Heever (1994) and Sigurdsen (2006). Based on our examination of this feature in *Lycosuchus* and other theriodonts, we agree with van den Heever (1994) that the posterior maxillary sinus in therocephalians is homologous with the maxillary antrum in cynodonts (e.g., Fourie, 1974; Crompton et al., 2017; Pusch et al., 2019). At the anteroventral tip of the maxillary antrum, a branching maxillary canal extends forwards, starting at the level of the root of the second canine and ending at the posterior margin of the premaxilla at the level of the root of the fifth incisor (**Figures 6**, **13C**). This maxillary canal would have housed the maxillary branch of the trigeminal nerve

(CNV_2), a branch of the facial nerve, and blood vessels (Benoit et al., 2016a). The caudal part of the maxillary canal, which is connected to the maxillary antrum, ramifies into two of the three branches for the alveolar rami of the CNV_2 (probably the caudal and medial alveolar rami), as in the baurioid *Choerosaurus dejageri* (Benoit et al., 2016b). Both rami radiate from the same point within the maxillary canal. As in *Choerosaurus*, the caudal part of the maxillary canal appears relatively long (Benoit et al., 2016a,b). Its diameter is generally larger than that of the rostral part of the canal, but narrows posteriorly where it disappears into the maxillary antrum (**Figure 6**). The rostral part of the maxillary
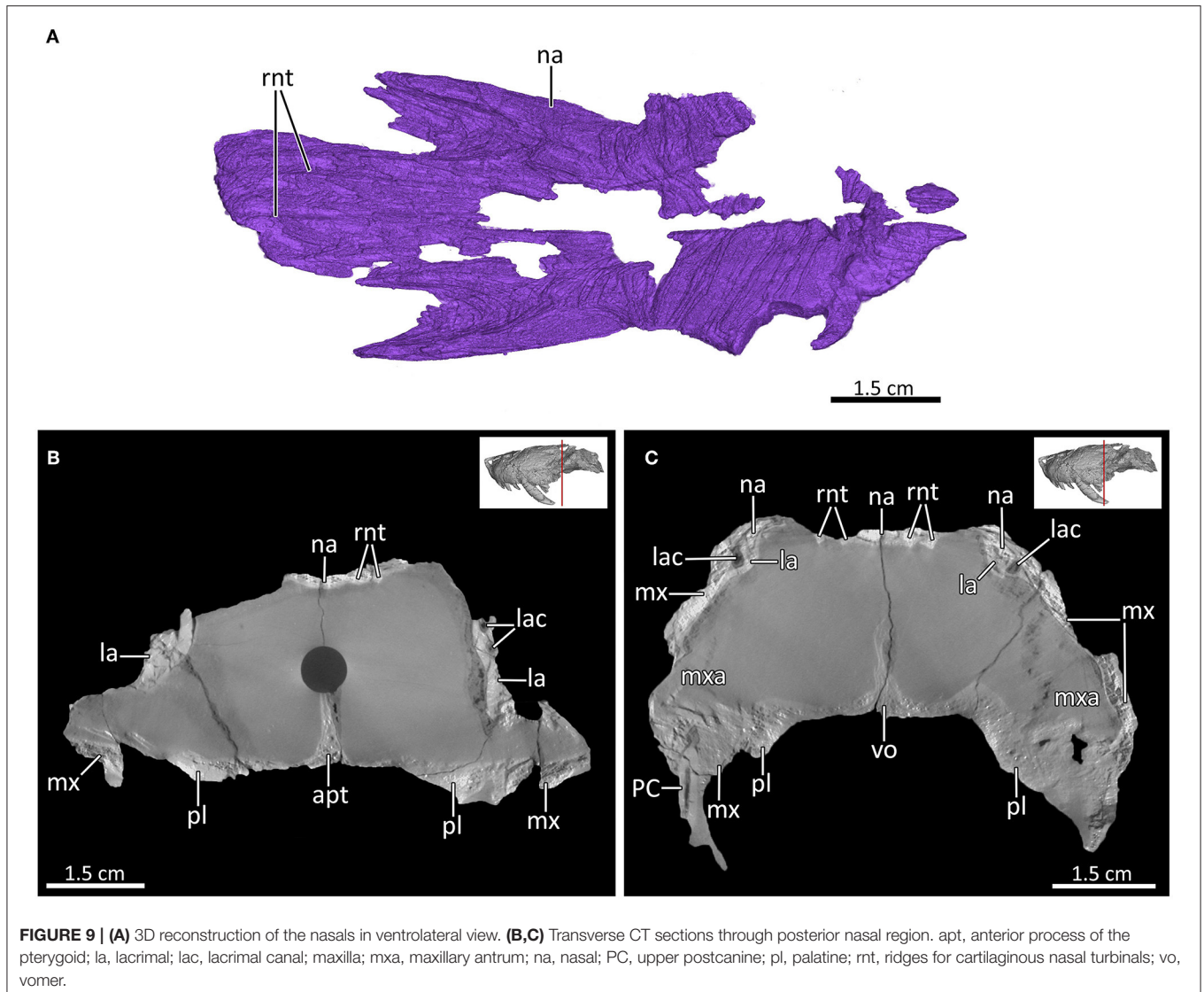
canal, which is the homolog of the tube for the infraorbital ramus (ION) (Benoit et al., 2016a) begins immediately anterior to the bifurcation of the alveolar rami. It is highly ramified in MB.R.995 with three main ramifications: the external nasal rami, internal nasal rami, and superior labial rami. At the posterior portion of the rostral part, a complex of canals for the external nasal rami of the ION diverge dorsally at the level of the root of the large C1, consisting of a long, nearly vertically-directed major ramus, which has a robust base within the maxillary canal and further smaller, strongly ramified anterodorsally-directed ramifications diverging ventrally near its base. Anterior to this complex there is a further small, anteriorly-directed canal for the external nasal ramus diverging from the main branch of the maxillary canal (**Figure 6**). Just anterior to the complex of external nasal rami, a narrow ramus diverges ventrally from the maxillary canal, which bears a small anteriorly-directed ventral ramification. This ramus might have housed the superior labial ramus of the ION. There are two further ventral ramifications for the superior labial rami diverging anterior to the ramified ventral ramus, consisting of a small anteroventrally-directed ramus and a long anteriorly-curved ramus near the anterior tip of the maxillary canal (**Figure 6**). The latter terminates anteriorly as an internal nasal ramus lateral to I5. Two further canals that probably housed internal nasal rami of the ION diverge dorsally from the maxillary canal toward the superior labial rami. The posterior one is small and anteriorly directed, whereas the anterior one curves anterodorsally (**Figures 6B,C**). A definite rostral alveolar canal cannot be discerned in this specimen. Benoit et al. (2019) recently discussed whether the posteriormost branch of the superior labial canal is homologous with the rostral alveolar canal of the CNV_2 in cynodonts; we consider this possible, but uncertain pending additional data on facial innervation in eutheriodonts.

The plate-like lacrimal is positioned at the anterior wall of the orbit. Both lacrimals are badly damaged. They show unusually expansive lateral exposure for a therocephalian, due to external wear to the snout surface exposing portions that normally would have been covered by the maxilla, prefrontal, and jugal (**Figures 2–4**, **7**, **9B**). In more intact skulls of *Lycosuchus*, the dorsal portion of the maxilla and the prefrontal exclude the lacrimal from contacting the nasal externally (Broom, 1903; van den Heever, 1987, 1994), as is the case in almost all therocephalians except lycideopids (e.g., Sigurdsen et al., 2012). However, since the prefrontal is not preserved in MB.R.995, the anterodorsal part of the lacrimal is exposed where it contacts the nasal internally. In this area, the lacrimal has a slender anterior process extending out from its anterodorsal portion onto the medial surface of the posteroventral margin of the nasal, which is overlapped by the maxilla laterally (**Figure 7**). An anterior process of the lacrimal contacting the nasal internally has also been described for akidnognathids (Sigurdsen, 2006), *Tetracynodon* (which has a relatively short anterior process; Sigurdsen et al., 2012), and is also observed in *Glanosuchus* (van den Heever, 1987, 1994; Hillenius, 1994). van den Heever (1987) questioned the presence of an anterior process of the lacrimal in Lycosuchidae, since this feature appeared absent in the specimen CGS C60. Later, van den Heever (1994) countered that

interpretation, stating that both scylacosaurids and lycosaurids possess an anterior process of the lacrimal, although still basing his conclusions on CGS C60, in which the lacrimal is damaged. Our reconstruction of MB.R.995 confirms van den Heever's (1994) inference that this feature is present in lycosuchids. On its medial surface, the lacrimal exhibits a distinct ridge, the lacrimo-palatine ridge, which contacts the dorsolateral margin of the palatine and forms the posterior border of the maxillary antrum (**Figures 6A**, **7**). The lacrimal has a further ridge, the lacrimo-ectopterygoidal ridge, which is posteroventrally oriented (van den Heever, 1987, 1994). This ridge is poorly preserved on the right lacrimal, which is more completely preserved posteriorly than the left, and contacts the dorsal process of the ectopterygoid and the posterolateral process of the palatine ventrally on the floor of the orbit (**Figures 2B**, **4B**, **7C**). Broom (1903) and van den Heever (1987, 1994) described a single lacrimal foramen in the anterior edge of the orbit in *Lycosuchus*. However, our CT-scans of MB.R.995 show that two foramina are present in the anterior region of the orbit (**Figure 9B**). Although the exact point where the canal opens anteriorly cannot be determined with certainty, it probably opened below the base of the anterior process of the lacrimal, above the maxillary antrum (**Figures 6A**, **7**, **9C**), as suggested by Sigurdsen (2006), rather than at the anteriormost tip of the anterior process as described by Hillenius (1994) for *Glanosuchus*. Hillenius (1994) described a further ridge in *Glanosuchus*, immediately anterior to the anterior process of the lacrimal and below the nasoturbinal ridge, that may have supported maxilloturbinals. In contrast, Sigurdsen (2006) proposed that maxilloturbinals were absent in therocephalians. No internal snout ridges other than those on the nasals (described above) can be observed in MB.R.995 (**Figure 7**), indicating that cartilaginous maxilloturbinals were probably not present in *Lycosuchus*.

Palate

The paired vomer is a broad, elongated element with a long interchoanal process (**Figures 7A,C**, **8**). This process expands anteriorly and becomes widest where it contacts the vomerine process of the premaxilla. In ventral view, the anterior process of the vomer is deeply vaulted. An equally long but much narrower trough is present on the dorsal surface of the interchoanal process. Anterior to this trough, the vomer tapers toward its tip, which overlies the vomerine process of the premaxilla (**Figure 8**). A slight median ridge separating two shallow grooves is present on this attenuate anteriormost part of the vomer (**Figure 8A**). Similar grooves on the dorsal surface of the vomer have been described for several therapsids and are interpreted as the location for a pair of vomeronasal organs (e.g., Hillenius, 2000; Crompton et al., 2017; Kammerer, 2017; Liu and Abdala, 2017; Bendel et al., 2018; Pusch et al., 2019). Posteriorly, where the vomer contributes to the posterior margin of the choana, the vomer becomes a broad plate-like element, which is bordered laterally by the palatine. At its posteriormost end, the vomer constricts in transverse width and terminates in a contact with the anterior process of the pterygoid. In dorsal view, the broadened posterior portion of the vomer appears to form two short "wings" that project laterally, overlying the

FIGURE 9 | (A) 3D reconstruction of the nasals in ventrolateral view. **(B,C)** Transverse CT sections through posterior nasal region. apt, anterior process of the pterygoid; la, lacrimal; lac, lacrimal canal; maxilla; mxa, maxillary antrum; na, nasal; PC, upper postcanine; pl, palatine; rnt, ridges for cartilaginous nasal turbinals; vo, vomer.

palatines (**Figures 7C, 8A**). This winged structure of the posterior portion of the vomer slightly resembles the condition described for cynodonts, in which the laterally directed wings form a transverse lamina with the transverse processes of the palatine (e.g., Crompton et al., 2015, 2017; Pusch et al., 2019). The dorsal surface of the posterior portion of the vomer has a median ridge that continues onto the anterior process of the pterygoid. Our reconstruction of the position of the vomerine-pterygoid suture is based on examination of the external surface of the specimen and comparisons with other lycosuchids, as this suture is indeterminable in our scans. The dorsal margin of this ridge bears a slight groove medially and might have supported the ventral edge of the cartilaginous nasal septum as suggested by van den Heever (1987, 1994), similar to the condition in cynodonts (Fourie, 1974; Crompton et al., 2015, 2017; Pusch et al., 2019). Lateral to the median ridge, there are a pair of more weakly-developed ridges, running anteromedially to posterolaterally on the wings of the vomer and slightly extending onto the dorsal

surface of the palatines, which are covered by the dorsal laminae of the maxillae in this area (**Figure 8A**, arrows).

The palatine is a large bone that forms much of the palate and consists of two portions, an anterior process and a raised posteromedial boss. The anterior process is narrow, contacting the canine boss of the maxilla laterally and the vomer medially. It forms the posterolateral margin of the choana (anteromedially) and the lateral borders of the maxillary sinus (posteriorly) and the maxillary antrum (further posteriorly). Close to its contact with the maxilla, its lateral portion is rugose and bordered by a distinct, medially-situated ridge, the palatine ridge, which stretches posteriorly until it contacts the dorsal margin of the suborbital vacuity. Anterior to the latter, the palatine is pierced by a pronounced posterior palatine foramen (**Figures 7A,C, 8B**). At the level of the posterior border of the maxillary antrum, the palatine contacts the lacrimo-palatine ridge of the lacrimal and widens to form the posteromedial boss, an elongated element that contacts the narrow posterior portion of the vomer and the

anterior process of the pterygoid medially, the anterior margin of the pterygoid posteromedially, and forms the anteromedial margin of the suborbital vacuity. The posteromedial bosses of the palatines and the anterior process of the pterygoid are slightly damaged in MB.R.995 due to a large crack starting anterolaterally on the left palatine and ending posterolaterally near the anteromedial margin of the right suborbital vacuity (**Figures 8**). The ventral surface of the posteromedial boss bears the anterior portion of the pterygo-palatine ridge, which extends onto the anteromedial portion of the pterygoid (**Figure 8B**). Posterolaterally, the palatine bears a posterolateral process (damaged on the left side), which contacts the anterior process of the ectopterygoid posteriorly, the posterior process of the lacrimal dorsally, and forms the anterolateral margin of the suborbital vacuity (**Figures 3B**, **4B**, **7A,C**, **8**). The dorsal surface of the palatine is generally flat and smooth (**Figure 8A**), but seems to be slightly concave medially.

The ectopterygoid is a narrow, vertically oriented strut situated at the lateral margin of the transverse flange of the pterygoid and forming the posterolateral margin of the suborbital vacuity. It bears three processes: a ventral process at the edge of the transverse flange of the pterygoid, an anterior process contacting the lateral process of the palatine, and a dorsal process contacting the poorly-preserved lacrimo-ectopterygoidal ridge of the right lacrimal (**Figures 2B**, **3B**, **4B**, **7A,C**, **8**). In dorsal view, the ectopterygoid only has a small, triangular exposure, since its dorsal surface is mostly covered by the lateral margin of the transverse flange of the pterygoid (**Figures 2B**, **8A**).

Only the anterior part of the pterygoid is preserved, consisting of a relatively long and slender anterior process and parts of the pterygoid transverse flanges. The anterior process extends between the posteromedial bosses of the palatines and contacts the narrow posterior end of the vomer (**Figures 2B**, **7A,C**, **8**). The dorsal surface of the anterior process exhibits a distinct median ridge, which extends from the posterior portion of the vomer and continues along the anterior portion of the pterygoid until it reaches a slight narrow slit posteriorly, separating the transverse processes (**Figures 8A**, **9B**). This slit probably represents the anterior opening of the interpterygoid vacuity, which extends posteriorly to the base of the processus cultrifomis of the parasphenoid (van den Heever, 1987, 1994). Such a median ridge on the dorsal surface of the anterior part of the pterygoid, which is continuous with that of the vomer, has also been described by van den Heever (1987, 1994) for basal therocephalians, Liu and Abdala (2017) for *Shiguaignathus*, and Sigurdsen (2006) for an indeterminate South African akidnognathid. The pterygoids form the posterior margin of the suborbital vacuity and define the posterior portion of the transverse process (**Figure 8**). This transverse process is usually dentigerous in *Lycosuchus*, bearing a row of teeth erupting directly from its ventral margin (van den Heever, 1987, 1994; Kammerer and Masyutin, 2018). However, these teeth are not preserved in MB.R.995.

Braincase
The prootic lies in front of the ear region and contributes to the anterior border of the inner ear and the sidewall of the braincase. It is bounded dorsally by the supraoccipital,
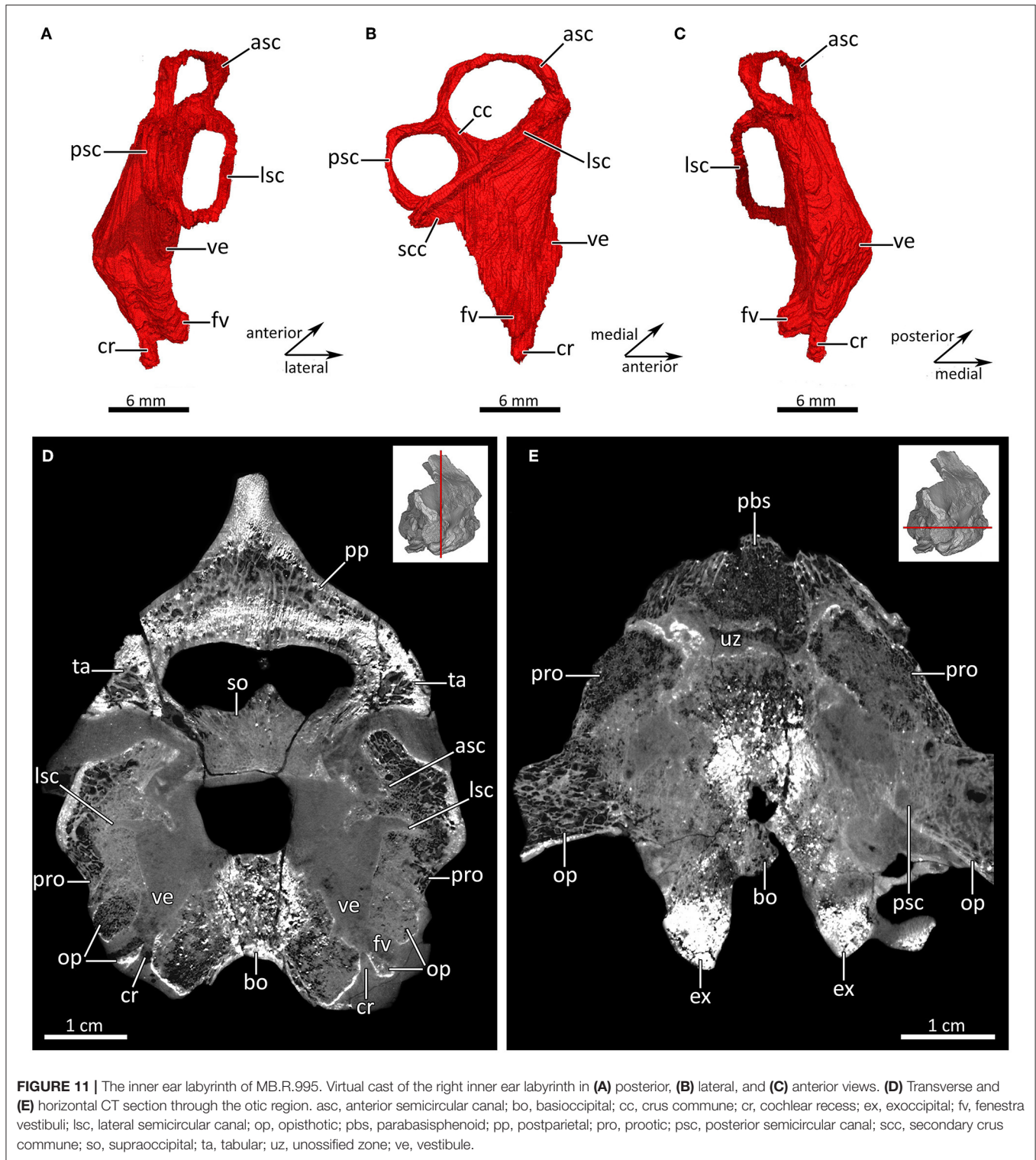
posterodorsally by the tabular, posteroventrally by the opisthotic, and anteroventrally by the basioccipital and the parabasisphenoid (**Figures 10B,C,E,F**, **11D,E**). Anteriorly and anterodorsally it would usually contact the epipterygoid (missing in this specimen) and posterolaterally the squamosal, which is only partly preserved in MB.R.995 (**Figures 10B,C,E**) (van den Heever, 1987, 1994). The anterior portions of the prootics, which broadly contact the posterodorsal part of the basisphenoid and the anterolateral portion of the dorsal surface of the basioccipital, curve medially and near (but do not contact) one another. The medial processes of the prootics form the lateral border of the small dorsum sellae of the basisphenoid, which occupies the narrow space between them (**Figures 10C,E**, asterisk). Lateral to the medial process, the prootic usually bears an elongated pila antotica, which extends anterodorsally (van den Heever, 1987, 1994). However, the pila antotica is not preserved in MB.R.995, since the anterior part of both prootics is slightly crushed and not completely preserved. The dorsal surface of the prootic is characterized by a distinct lateral flange, which curves posterolaterally toward the supraoccipital and tabular and contacts them (**Figures 10B,C,E**). In scylacosaurids and eutherocephalians, the lateral flange of the prootic encloses, together with the prootic process of the squamosal, the pterygo-paroccipital foramen. This foramen and a prootic process of the squamosal are absent in lycosuchids (e.g., van den Heever, 1987, 1994; Huttenlocker et al., 2011; Huttenlocker and Abdala, 2015; Huttenlocker and Sidor, 2016).

Only parts of the posterior portion of the fused parabasisphenoid complex are preserved. The dorsal surface of this portion is almost completely covered by the anterior portion of the prootics. At its posteriormost part, the small dorsum sellae is situated at the suture with the basioccipital, immediately in front of a narrow unossified space, the unossified zone (**Figures 10E**, **11E**) mentioned by Olson (1944). The dorsum sellae is laterally bordered by the medial processes of the anterior part of the prootics and forms the posterior border of a shallow depression, the sella turcica, which housed the hypophysis. However, the sella turcica is only poorly preserved in MB.R.995 (**Figures 10C,E**). In ventral view, the parabasisphenoid meets the basioccipital posteriorly in a jagged suture and simultaneously overlaps much of its anterior part. In addition, the parabasisphenoid contributes to the anterior margin of the cochlear recess (**Figure 10F**).

The basioccipital is a short, stout bone, which forms the floor of the braincase posterior to the parabasisphenoid and part of the occipital condyle. Its dorsal surface is anterolaterally almost completely covered by the medial processes of the anterior portions of the prootics, which leave only a narrow space posterior to the dorsum sellae. Posterior to the medial processes of the prootics, the dorsal surface of the basioccipital is marked by a slight depression, which contributes to the floor of the hindbrain region. Laterally, it contacts the opisthotic and posterolaterally the exoccipital, which covers much of its dorsal surface in that area, so that the basioccipital just appears as a narrow strip of bone posteriorly (**Figures 10B–F**, **11D,E**). Only a small portion of the basioccipital is visible in occipital
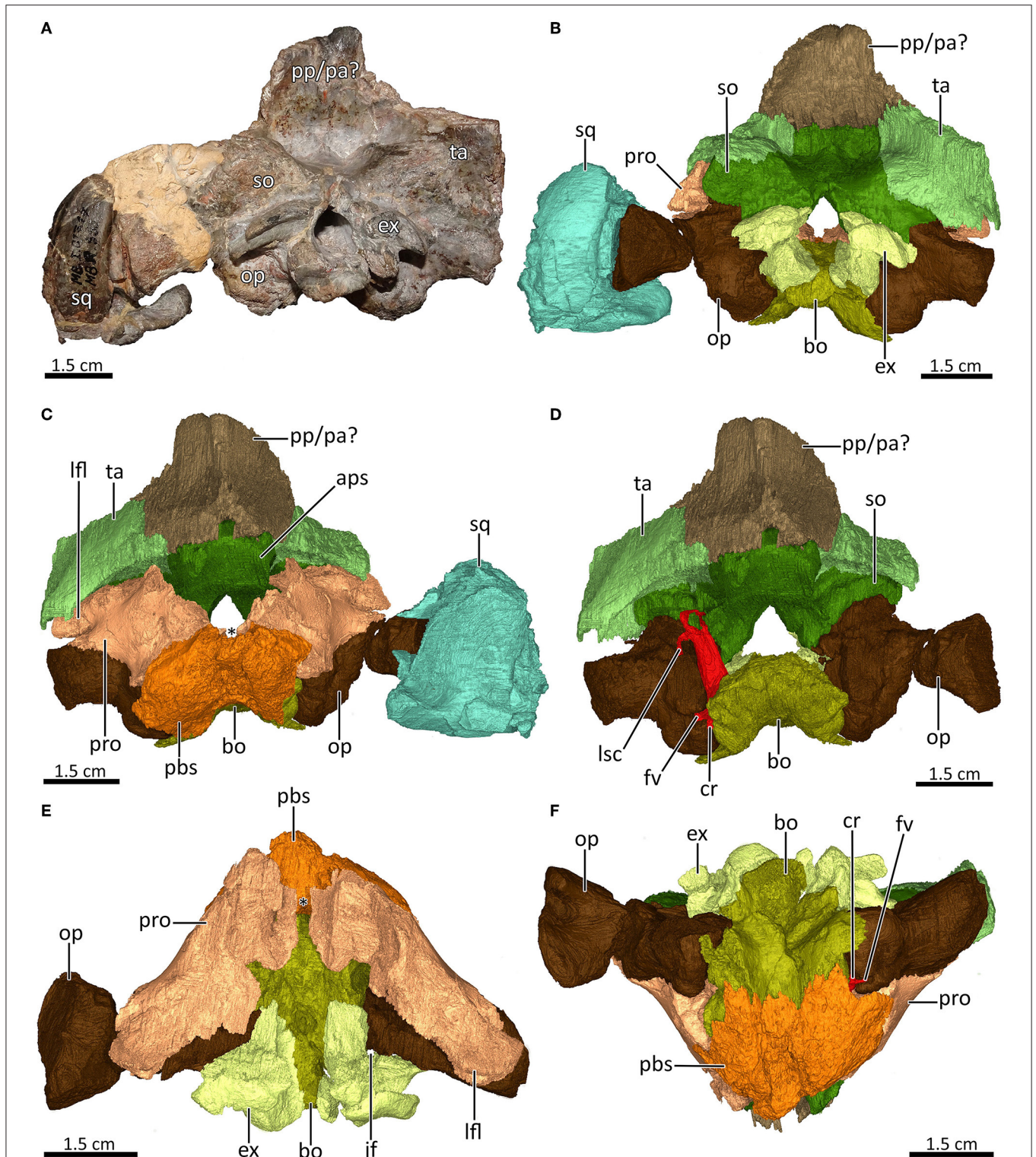
FIGURE 10 | Braincase of MB.R.995. **(A)** Photograph of the partial braincase in posterior view. **(B)** Posterior view of the reconstructed occiput. **(C)** 3D reconstruction of the braincase in anterior view. Asterisk indicates the location of the dorsum sellae. **(D)** Anterior view of the reconstructed occiput to illustrate the position of the inner ear within its bony housing with the parabasisphenoid, prootic and squamosal digitally removed. **(E)** Reconstructed braincase in dorsal and **(F)** ventral aspect, with the squamosal, tabular, supraoccipital, postparietal and parietal digitally removed in **(E)** and the squamosal digitally removed in **(F)**. Asterisk indicates the location of the dorsum sellae in **(E)**. aps, anterodorsal process of the supraoccipital; bo, basioccipital; cr, cochlea recess; ex, exoccipital; fv, fenestra vestibuli; jf, jugular foramen; lfl, lateral flange of the prootic; lsc, lateral semicircular canal; op, opisthotic; pa, parietal; pbs, parabasisphenoid; pp, postparietal; pro, prootic; so, supraoccipital; sq, squamosal; ta, tabular.

FIGURE 11 | The inner ear labyrinth of MB.R.995. Virtual cast of the right inner ear labyrinth in **(A)** posterior, **(B)** lateral, and **(C)** anterior views. **(D)** Transverse and **(E)** horizontal CT section through the otic region. asc, anterior semicircular canal; bo, basioccipital; cc, crus commune; cr, cochlear recess; ex, exoccipital; fv, fenestra vestibuli; lsc, lateral semicircular canal; op, opisthotic; pbs, parabasisphenoid; pp, postparietal; pro, prootic; psc, posterior semicircular canal; scc, secondary crus commune; so, supraoccipital; ta, tabular; uz, unossified zone; ve, vestibule.

view, forming the ventral border of the foramen magnum (**Figures 10B–D**). The ventral surface of the basioccipital is slightly damaged. It is concave medially but becomes convex laterally, with a process that slightly curves around the ventromedial margin of the opisthotic and contributes to the medial border of the cochlear recess (**Figures 10B–D,F**, **11D**).

The opisthotic consists of a robust paroccipital process, which is crushed on both sides. The right paroccipital process lacks much of its lateral portion, while the left one is more complete but is marked by a large crack and lacks part of its ventral portion. The lateral margin of the left opisthotic is concave and lies in a medially facing fossa of the squamosal.

Anterodorsally, the opisthotic broadly contacts the prootic, and posteromedially it has a sutural contact with the exoccipital above the jugular foramen housing cranial nerves IX, X, and XI, of which it forms the lateral margin. Its medial portion contacts the basioccipital, where its ventral margin is slightly overlapped by the lateral process of the latter. The opisthotic also forms the posterior and lateral border of the inner ear and cochlear recess and encompasses the fenestra vestibuli (**Figures 10, 11D,E**).

The supraoccipital appears as a broad element in occipital view, which forms the dorsal border of the foramen magnum. Ventrolaterally, it contacts the dorsal process of the opisthotic, ventrally the exoccipital, dorsolaterally the tabular, and dorsally the postparietal. However, the dorsal surface of the occiput is badly damaged and incomplete, leaving some uncertainties concerning the sutures between the supraoccipital, tabular, and postparietal (**Figures 10A,B, 11D**). The tabular usually covers part of the supraoccipital, but is damaged on the left side such that much of the underlying supraoccipital is visible. In anterior view, the supraoccipital contacts the dorsal portion and part of the lateral flange of the prootic. The internal surface of the supraoccipital is generally smooth, forming the roof of the posterior region of the brain cavity and the foramen magnum. It bears an anterodorsal process that contributes to the side wall of the braincase and contacts the parietal, prootic, and usually also the squamosal and the epipterygoid (van den Heever, 1994) (**Figures 10C,D**).

The paired exoccipitals form the lateral portion of the foramen magnum and the occipital condyle. The exoccipital has an expanded dorsal process forming sutures with the supraoccipital dorsally and the paroccipital process of the opisthotic laterally. Ventrally, it has a long lateral process that meets the posterolateral margin of the basioccipital laterally and the posterior part of the paroccipital process dorsomedially, forming the dorsal and medial margins of the jugular foramen (**Figures 10A,B,E,F, 11E**).

The paired tabulars are flat bones forming the dorsolateral portion of the occiput. Both tabulars are damaged, but the right one is better preserved, while the left tabular lacks portions that would otherwise cover the underlying supraoccipital. Dorsally and dorsolaterally, the tabular contacts the postparietal and the parietal, and medially the supraoccipital. Laterally, the tabular usually supports the squamosal in better preserved skulls, and between the foramen magnum and the posterodorsal margin of the post-temporal fenestra, the tabular usually exhibits a ridge (van den Heever, 1987, 1994). However, the tabular ridge is not preserved in MB.R.995 due to poor preservation. In anterior view, the tabular has a process that extends ventrolaterally and contacts the lateral flange of the prootic (**Figure 10C**).

The dorsal portion of the occiput is badly damaged, but the large complex of bones at its top probably consists of both postparietal and parts of the parietal (**Figures 9A–D, 10D**). The postparietal is a median element, which is situated within a large depression where it is bounded between the parietal dorsally, the tabulars laterally and the supraoccipital ventrally. There seems to be a weakly preserved median ridge on the posterior surface of the bone, which divides the depression into two nuchal fossae (**Figures 10A–D**).
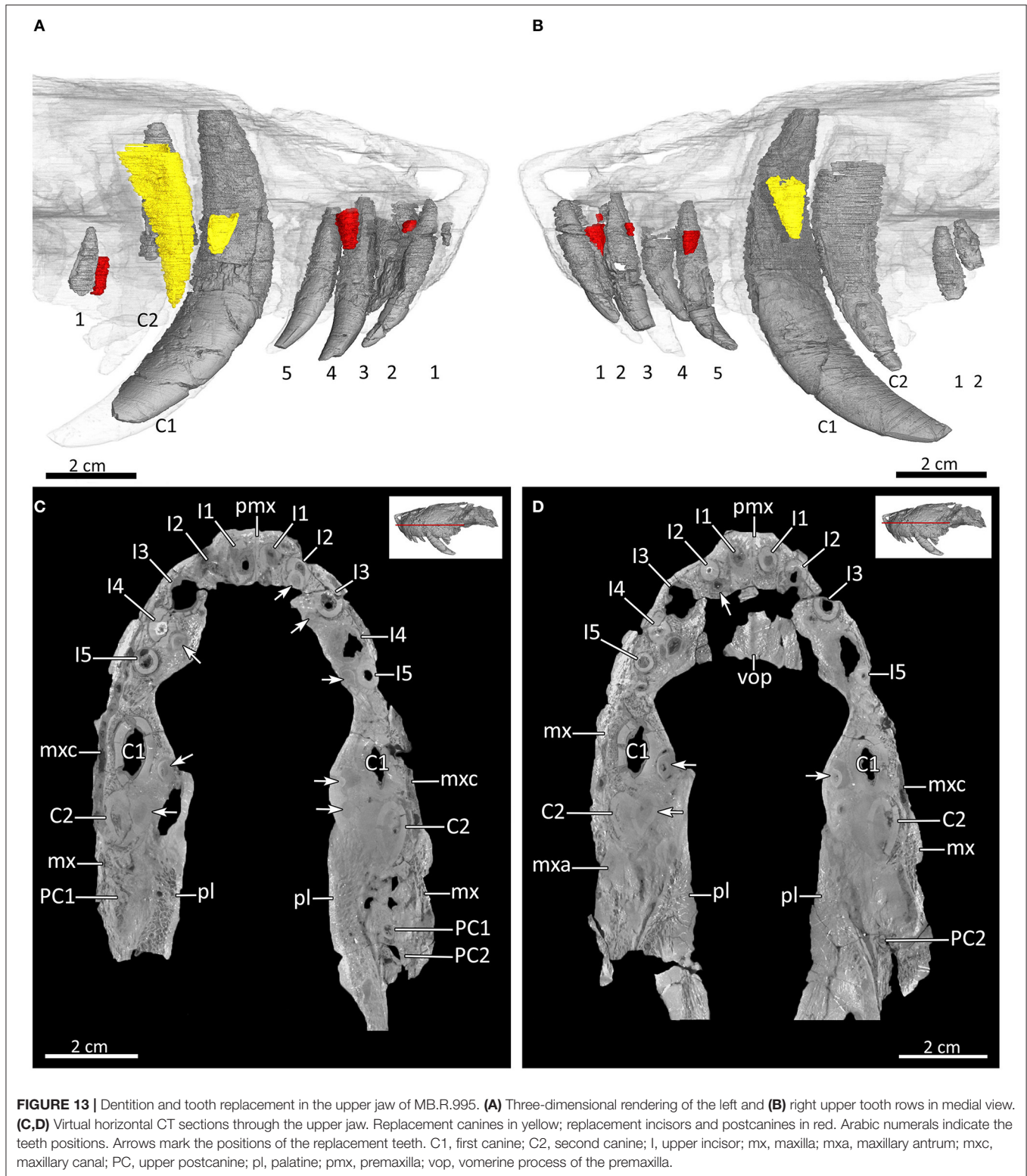
The left squamosal is only partially preserved, where it forms the posterolateral portion of the temporal region. It lacks several parts: e.g., the dorsal process that overlies the parietal dorsolaterally, the quadrate process, and the anterolaterally located zygomatic process, which overlies the posterior portion of the jugal (**Figures 10B,C**) (van den Heever, 1987, 1994). The squamosal bears a medially-located fossa for the paroccipital process of the opisthotic. On its posterior surface the dorsoventrally directed squamosal sulcus seems to be preserved, which is medially bordered by the squamosal ridge lateral to its contact with the opisthotic (**Figures 10B,C**).

Inner Ear

As in other therapsids, multiple bones of the basicranium contribute to the formation of the inner ear housing in MB.R.995, consisting of the opisthotic, prootic, supraoccipital, exoccipital and basioccipital (**Figures 10C,D,F, 11C,D**) (e.g., Olson, 1944; Fourie, 1974; Sigogneau, 1974; Luo et al., 1995; Luo, 2001; Kielan-Jaworowska et al., 2004; Pusch et al., 2019). At greatest height, the inner ear of MB.R.995 is 22.95 mm tall. Its semicircular canals are surrounded by the exoccipital, supraoccipital, opisthotic, and prootic. Medially, both anterior and posterior semicircular canals derive from the crus commune, where they emerge dorsally at the same level from its posterior apex and curve downward to join the anterior and posterior ampullar recess, respectively. The posterior semicircular canal is smaller than the anterior with a height of 6.20 mm and a width of 5.52 mm, while the anterior canal is 7.21 mm tall and 7.69 mm wide. The lateral (horizontal) semicircular canal appears to be the longest of the three semicircular canals, with a height of 3.81 mm and a width of 10.88 mm (**Figures 10C,D, 11**). This situation is unusual, because in most non-mammalian therapsids and mammals the anterior semicircular canal is the longest (e.g., Olson, 1944; Sigogneau, 1974; Luo, 2001; Kielan-Jaworowska et al., 2004; Rodrigues et al., 2013; Laaß, 2016; Araújo et al., 2017, 2018; Benoit et al., 2017b,c; Bendel et al., 2018; Pusch et al., 2019). Among therapsids, a lateral semicircular canal larger than the anterior and posterior one has only previously been reported for the fossorial anomodont *Kawingasaurus fossilis* (Laaß, 2015a). The lateral and posterior canal share a secondary crus commune (**Figure 11B**), as in most non-mammalian therapsids (e.g., Olson, 1944; Sigogneau, 1974; Castanhinha et al., 2013; Rodrigues et al., 2013; Laaß, 2015a, 2016; Araújo et al., 2017, 2018; Benoit et al., 2017b,c; Bendel et al., 2018; Pusch et al., 2019). The curved vestibule has a length of 13.59 mm and is surrounded by the opisthotic and the prootic, of which the opisthotic constitutes its posterior and lateral border and the prootic its anterior border. The fenestra vestibuli faces ventrolaterally and is exclusively bordered by the opisthotic. Of particular note is the presence of a small, globular cochlear recess, which is ventrally differentiated from the main part of the vestibule and located medial to the fenestra vestibuli. It is posteriorly bordered by the opisthotic and medially bordered by the basioccipital (**Figures 10C,D,F, 11A–D**). The parabasisphenoid also indirectly contributes to the anterior margin of the cochlear
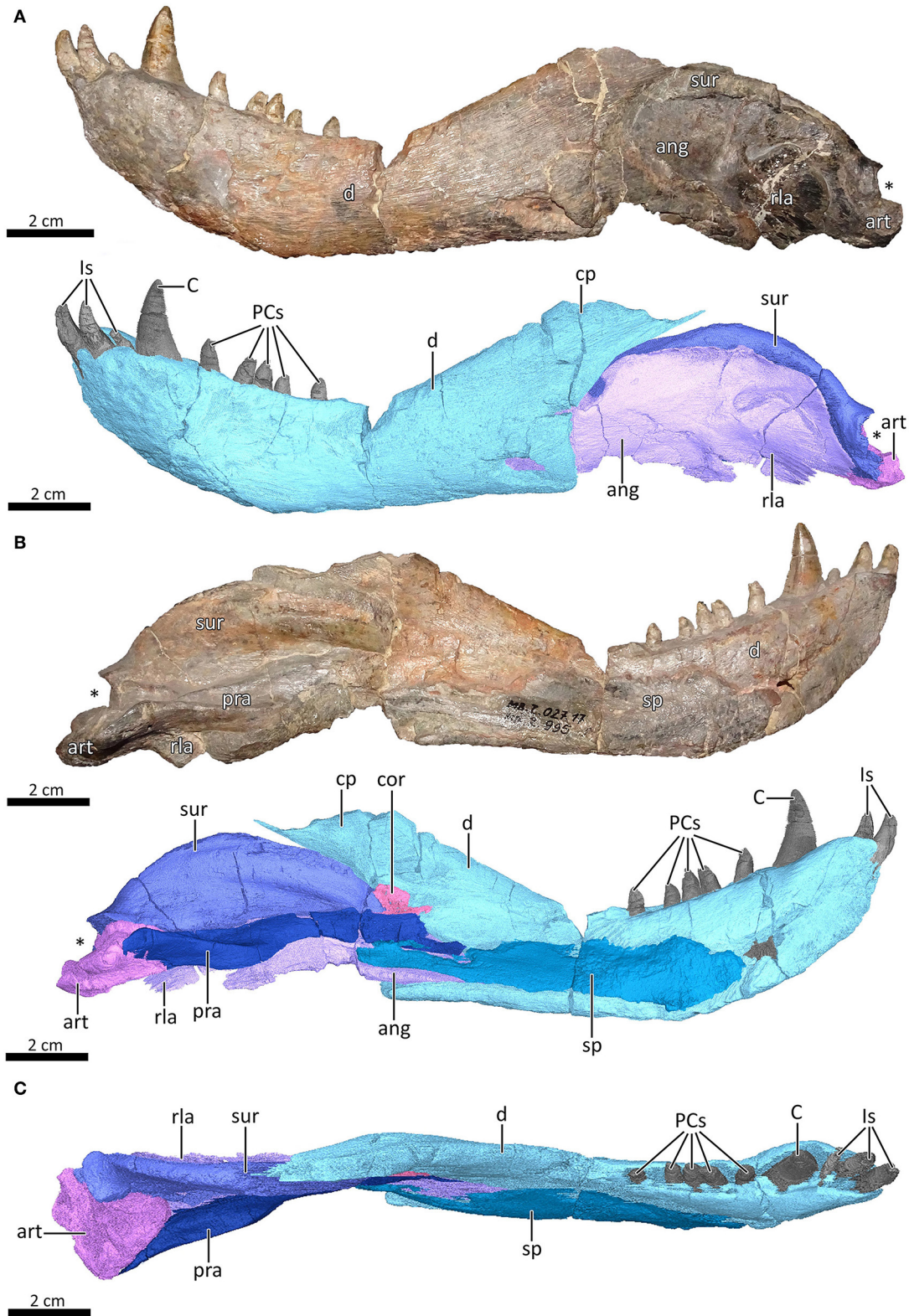
FIGURE 12 | Left mandible of MB.R.995. **(A)** Photograph (top) and 3D reconstruction (bottom) of the left mandible in lateral view. **(B)** Photograph (top) and 3D reconstruction (bottom) of the left mandible in medial view. **(C)** Dorsal view of the reconstructed left mandible. Asterisk indicates the location of the glenoid fossa. ang, angular; art, articular; C, lower canine; cor, coronoid; cp, coronoid process; d, dentary; ls, lower incisors; PCs, lower postcanines; pra, prearticular; rla, reflected lamina of the angular; sp, splenial; sur, surangular.

FIGURE 13 | Dentition and tooth replacement in the upper jaw of MB.R.995. **(A)** Three-dimensional rendering of the left and **(B)** right upper tooth rows in medial view. **(C,D)** Virtual horizontal CT sections through the upper jaw. Replacement canines in yellow; replacement incisors and postcanines in red. Arabic numerals indicate the teeth positions. Arrows mark the positions of the replacement teeth. C1, first canine; C2, second canine; I, upper incisor; mx, maxilla; mxa, maxillary antrum; mxc, maxillary canal; PC, upper postcanine; pl, palatine; pmx, premaxilla; vop, vomerine process of the premaxilla.

recess by overlapping the basioccipital (**Figure 10F**). Among therocephalians, a distinctive cochlear recess has so far only been described in the specialized baurioid *Microgomphodon oligocynus* (Benoit et al., 2017b).

Lower Jaw

The left mandible of MB.R.995 consists of seven bones: the dentary, splenial, angular, surangular, one coronoid (likely homologous to the posterior coronoid in early tetrapods

[*sensu* Ahlberg and Clack, 1998]), prearticular and articular. The dentary represents its largest element, composing roughly two-thirds of the anteroposterior jaw length (**Figure 12**). The lateral surface of the dentary is smooth up until the region below the canine, then becomes rugose on the symphysis. The mandibular symphysis was interpreted by van den Heever (1987, 1994) as a relatively loose contact—a feature that sets apart therocephalians from gorgonopsians and cynodonts. In eucynodonts the dentaries are fused at the symphysis (Hopson and Kitching, 2001), but even in earlier cynodonts where the dentaries remain separate elements they are tightly sutured. Anteriorly, the dentary is swollen laterally, with the greatest expansion positioned at the level of the canine (**Figure 12C**). A pronounced shelf runs medially along the tooth row. The ventral margin of the dentary is generally flat, in contrast to the gradually sloping ventral margin in Gorgonopsia and later Therocephalia (van den Heever, 1987, 1994). At the symphysis, it curves gently upwards anteriorly, unlike the sharply-sloping symphysis in Gorgonopsia. Posteriorly, the dentary terminates at a near-perpendicular angle to the vertical posterior margin, which curves smoothly posterodorsally to form the free-standing edge of the coronoid process (**Figure 12A**). A substantial portion of the medial dentary surface is covered by the splenial, resting on an anteroposteriorly directed gutter (**Figure 12B**), which together cover the Meckelian canal (van den Heever, 1987, 1994). Posteriorly, the dentary articulates with the angular and the surangular at the same point. Part of the anterior portion of the angular is visible through a crack at the dentary angle. The base of the coronoid process is posteromedially covered by the anteriormost part of the prearticular and the coronoid.

The splenial is present as an anteroposteriorly elongate element positioned medial to the dentary, extending from the root of the canine to a level in line with the apex of the coronoid process (**Figures 12B,C**). It has no lateral exposure. The dorsoventral height of the splenial is roughly conserved through its length, but does decrease slightly posteriorly, similar to what has been described for *Gorynychus* (Kammerer and Masyutin, 2018). According to van den Heever (1987, 1994), the splenial contributes to the symphysis in early therocephalians. As only the splenial of the left hemimandible is well-preserved in MB.R.995 and the posterior symphyseal region is slightly damaged, this condition can neither be confirmed nor disputed for this specimen. At its posterior end, the splenial medially overlies the anteriormost portion of the angular and the anteroventral part of the prearticular (**Figure 12B**).

The angular is a transversely thin, dorsoventrally tall bone positioned posterior to the dentary and is mostly exposed laterally (**Figures 12A,B**). Its ventral margin is somewhat damaged, but the lateral surface is intact. In lateral view, the angular obscures most of the surangular. The reflected lamina covers the posterior half of the angular. It is smooth and well-developed, forming a roughly circular, thin sheet of bone that, as a result of diagenesis, is closely pressed against the main body of the angular (**Figure 12B**). The ridges on the lateral surface of the reflected lamina could not be discerned in our reconstruction, but have been described in MB.R.995 by Janensch (1952). The angular is embedded in and supported anteriorly by a trough in the posteroventral margin of the dentary, where it is further covered medially by the splenial and the prearticular. Posteriorly, it supports the ventral part of the articular.

The surangular forms the posterodorsal region of the mandible, curving smoothly toward the glenoid fossa and forming a strongly convex dorsal surface (**Figures 12A,B**). It is a fairly robust bone, equal in width to the dentary that lies against the medial side of the angular. The angular covers most of the surangular in lateral view, leaving only a thin, sickle-shaped strip visible (**Figure 12A**). In MB.R.995, the ventral margin of the surangular is slightly damaged. A postdentary foramen between the surangular and prearticular has been described in US D173 (van den Heever, 1987), but could not be confirmed for MB.R.995. Anteriorly, the bone narrows dorsoventrally until it touches the dentary, where it is also covered medially by the coronoid and prearticular. At the posterior end, it overlies the dorsal part of the articular. At this contact, the surangular widens mediolaterally to form the dorsal roof of the glenoid fossa (**Figures 12A,B**, asterisk).

A small, flat and roughly triangular-shaped bone that sits medially to the base of the coronoid process of the dentary is interpreted as representing the coronoid bone (**Figure 12B**). The coronoid has not been described in US D173 (Broom, 1903), and is typically damaged, obscured or missing in other therocephalians. The coronoid cannot be seen in the ventral view of the jaw, unlike the condition in *Microgomphodon* (Abdala et al., 2014b). The coronoid borders the anterodorsal part of the prearticular and covers the anterior portion of the surangular and the posteroventral portion of the coronoid process of the dentary medially (**Figure 12B**).

The prearticular is an elongated strut, extending from the posterior part of the dentary to meet the anteromedial side of the articular (**Figure 12B**). It lies medially to the angular and ventral part of the surangular. Anteriorly, it defines the ventral margin of the coronoid, and it is overlain medially by the posterodorsal portion of the splenial. A small process extends anteriorly to contact the base of the coronoid process of dentary. Posteriorly, at the level of the apex of the surangular, a medial expansion is present (**Figures 12B,C**), ultimately terminating at a posteromedially oriented suture with the articular. An anteroposteriorly-oriented fossa on the dorsal surface of the prearticular is located anterior to this suture (**Figure 12C**).

The articular is the posteriormost element of the mandible, and bears the ventral and anterior boundaries of the glenoid fossa (**Figures 12A,B**). In MB.R.995, a fragment of the quadrate seems to be preserved inside the left glenoid. The articular is a robust bone, extending significantly beyond the dentary medially in an extended contact with the prearticular (**Figure 12C**). Anterolaterally, it contacts the posterior portions of the surangular and angular.

Dentition and Tooth Replacement

The teeth in the left dentary are generally well-preserved, while those in the upper jaw are mostly damaged, albeit slightly better preserved on the right side than on the left. All teeth in both the

upper jaw and the left dentary are preserved in place, except for the first incisor of the left premaxilla, which has fallen out with only a fragment of its root preserved in its alveolus (**Figures 3**, **4**, **7**, **8B**, **12–14**). Serrations are probably present on both the mesial and distal margins of all teeth (**Figures 13A,B**, **14A**) (see also van den Heever, 1987, 1994), although damaged on much of the upper dentition in MB.R.995.

MB.R.995 has five upper and three lower incisors. They have a simple conical shape and are slightly recurved, except for the third lower incisor, which is markedly smaller than all other incisors (**Figures 3**, **4**, **6D**, **7**, **8B**, **12–14**). The upper incisors are located in a broad ventral plate of the premaxilla (**Figures 7**, **8B**). van den Heever (1987, 1994) related incisor size in *Lycosuchus* to the height of the premaxilla at each tooth position, noting an increase in size from the first to the fourth upper incisor, which lies at a point where the bone is deepest, then a decrease in size to the fifth tooth, which is the smallest. In MB.R.995, there is indeed an increase in upper incisor size from the first to the fourth, but this is probably not related to the height of the premaxilla, as the premaxilla is not appreciably deeper at the position of the fourth incisor than anteriorly (**Figures 7**, **8B**). There are replacement teeth for upper incisors two and four on both sides, and for the upper third and fifth incisors on the right side. The replacement teeth are located either posterior (I2) or medial (I3, I4, I5) to the functional tooth. There is a coalescence between the alveoli of the functional and replacement teeth of the right I2 and the left I4, with the new incisor for I2 penetrating the root, and the new tooth for I4 eroding the root of the functional incisor. No evidence of replacement teeth or replacement pits can be observed for the first incisors on both sides and the third and fifth incisor on the left side (**Figure 13**). In the left dentary there are replacement teeth for all three lower incisors, which are positioned posterior to the functional teeth. The replacement teeth of I1 and I3 are still incipient, while that of I2 is much better developed. There is also a marked coalescence between the alveoli of the functional and replacement teeth, with the big replacement tooth behind I2 eroding the root of the functional tooth (**Figures 14A–C**).

Each maxilla bears an anterior and posterior canine alveolus. The anterior canines are fully erupted on both sides of the skull and are very large and nearly crescent-shaped. The right anterior canine is well-preserved; the left is broken at several places along its length and lacks the tip. A posterior canine is located immediately behind and slightly lateral to the anterior one in the right maxilla. The right posterior canine is not fully developed (the root has not fully formed) and its crown is only partially erupted (**Figures 3**, **4**, **6D**, **7**, **8B**, **13**). The root of a posterior canine is also present in the left maxilla, but its crown is missing entirely. Two unerupted developing canines are present in the left maxilla: a small, poorly-developed canine tip is present medial to the anterior canine and a large, well-developed tooth (consisting of most of the crown) is present medial to the broken posterior canine root. The incipient left anterior replacement canine has not yet eroded the root of the erupted canine. By contrast, the incipient left posterior replacement canine has penetrated the root of the old posterior canine tooth and is almost erupted. The anterior canine in the right maxilla has a medially located

replacement tooth as well, which is comparable in proportions and state of development to its counterpart on the left. The posterior canine alveolus in the right maxilla is not fully occupied by the erupting tooth, indicating that the previous tooth was shed and the erupted canine is the replacing tooth in the process of development (**Figure 13**). The lower canine has a broader base than the upper canines and is only weakly recurved (**Figures 12**, **14**). There is no replacement tooth visible for the lower canine, only the remnant of an older canine root is present anterior to the functional one, which nearly contacts the root of the lower i2 (**Figure 14**).

MB.R.995 has two upper postcanines in the right maxilla but only one postcanine in the left maxilla. By contrast, in the dentary there are five postcanines present. The postcanines are simple, conical teeth (Broom, 1903), with the uppers smaller than the lowers (**Figures 2**, **6D**, **7A,B**, **8B**, **13**). Only the single upper postcanine in the left maxilla is paired with a replacement tooth, which is anteromedially situated to the functional tooth. In the dentary there are incipient replacement teeth for lower postcanines one, three, and four, which are located either medial (PC1, PC3) or posteromedial (PC4) to the functional tooth. There is a coalescence between the alveolus of the replacement tooth of PC3 and the functional one. However, the replacement tooth does not erode the root of the functional PC3 (**Figures 13**, **14A,C,D**).

DISCUSSION

Maxillary Canal Evolution

The morphology of the maxillary canal of *Lycosuchus vanderrieti* reinforces the idea that homoplasy and mosaic evolution are major features of the evolutionary history of this structure in therapsids, as previously suggested based on the condition in the basal cynodont *Galesaurus planiceps* (Pusch et al., 2019). In comparison to eutherocephalians such as the akidnognathid *Olivierosuchus* and the bauriid *Bauria,* in which the maxillary antrum is anteroposteriorly extensive (Benoit et al., 2016a, 2018), the maxillary antrum of *Lycosuchus* is relatively small and restricted to a region anteroventral to the orbit. Comparable variation in maxillary antrum size is observed in cynodonts, where this structure is substantially greater in relative volume and anteroposterior extent in gomphodonts than in stemward cynodonts and probainognathians (Crompton et al., 2015, 2017; Benoit et al., 2016a, 2019; Pusch et al., 2019). Within-clade variation in maxillary antrum size seems to reflect differing degrees of ossification of the snout rather than differences in length of the nerves and vessels within—a shorter caudal portion of the maxillary canal appears to be present in cynodonts compared to therocephalians and gorgonopsians regardless of antrum dimensions. As in other non-cynodont therapsids (Benoit et al., 2016a,b, 2017a,c, 2018, 2019), the alveolar rami ramify directly from the maxillary canal and not from the maxillary antrum in *Lycosuchus*. Like the bauriod therocephalian *Choerosaurus*, only two of the three branches for the alveolar rami are present, which probably represent the caudal and medial alveolar rami. However, unlike in *Choerosaurus*, these rami in *Lycosuchus* radiate from the same point within the caudal part of the maxillary canal. This also occurs in *Olivierosuchus*, but in that
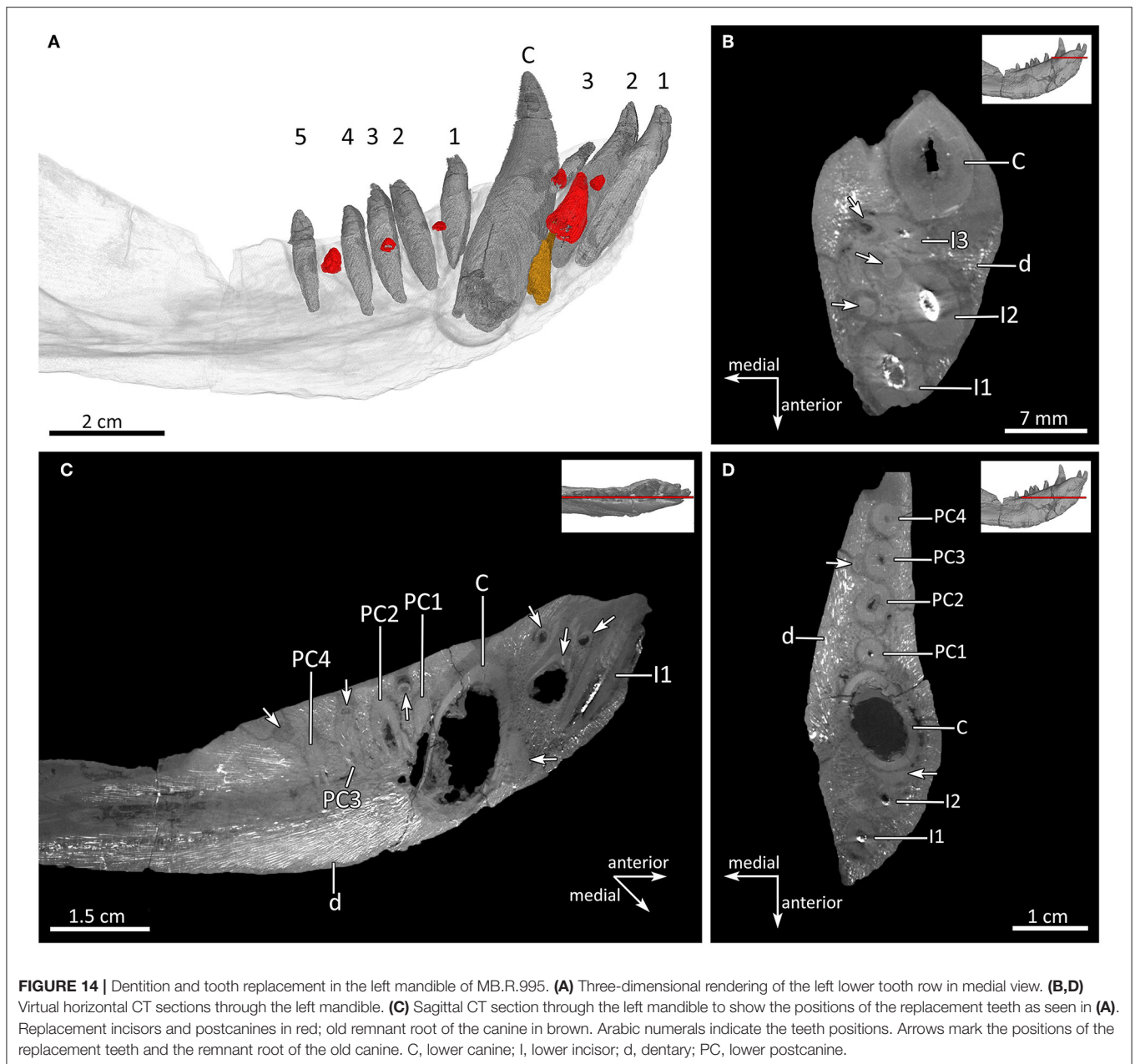
FIGURE 14 | Dentition and tooth replacement in the left mandible of MB.R.995. **(A)** Three-dimensional rendering of the left lower tooth row in medial view. **(B,D)** Virtual horizontal CT sections through the left mandible. **(C)** Sagittal CT section through the left mandible to show the positions of the replacement teeth as seen in **(A)**. Replacement incisors and postcanines in red; old remnant root of the canine in brown. Arabic numerals indicate the teeth positions. Arrows mark the positions of the replacement teeth and the remnant root of the old canine. C, lower canine; I, lower incisor; d, dentary; PC, lower postcanine.

taxon there is also a rostral alveolar ramus diverging just anterior to the caudal and medial alveolar rami (Benoit et al., 2016a,b, 2018).

The morphology of the external nasal ramus in *Lycosuchus* differs from that known in later-diverging therocephalians. In *Lycosuchus*, the external nasal ramus is highly ramified and forms a complex at the posterior part of the ION. Of particular note is the morphology of the lengthened major ramus, which resembles that of the external nasal ramus in the dinocephalian *Moschops* (Benoit et al., 2017c) and the anomodont *Patranomodon* (Benoit et al., 2018). However, in those taxa the ramus extends far posterodorsally toward the orbit, unlike in *Lycosuchus* in which the ramus is nearly

vertical. In the eutherocephalians *Choerosaurus*, *Euchambersia*, *Olivierosuchus*, and *Bauria*, the external nasal rami ramify into three or more branches, but they do not form the pronounced lengthened ramification of *Lycosuchus* (Benoit et al., 2016a,b, 2017a, 2018). Based on its shared presence in the earliest therocephalians and cynodonts, the highly ramified complex of canals for the external nasal rami in *Lycosuchus* likely represents the primitive condition. A more derived condition is present in some derived therocephalians such as *Olivierosuchus* and non-probainognathian cynodonts, in which the external nasal ramus is shorter and less ramified than in *Lycosuchus*. A further reduction of the external nasal ramus, associated with a reduction of the canals for the internal nasal

and superior labial rami, is only present in Probainognathia (Benoit et al., 2016a, 2018, 2019; Pusch et al., 2019).

Benoit et al. (2019) recently reinterpreted the short canal directed toward the base of the canine in the probainognathian *Ecteninion* as the canal for the rostral alveolar ramus, based on the fact that in mammals this ramus is consistently oriented toward the upper canine. A similar morphology is also observed in the maxillary canal of the basal cynodont *Galesaurus*, in which there is a slender ramus directed toward the upper canine, just anterior to the external nasal rami, which has also been interpreted as the rostral alveolar ramus (Pusch et al., 2019). This is similar to what is seen in *Lycosuchus*, but the narrow ramus just anterior to the complex of external nasal rami, diverging ventrally from the maxillary canal, is here interpreted as part of a complex superior labial ramus that has several origins from the main branch of the maxillary canal. The course of the maxillary canal in *Lycosuchus* differs from that described in most other therocephalians and therapsids (Fourie, 1974; Benoit et al., 2016a,b, 2017a,c, 2018, 2019; Pusch et al., 2019). The maxillary canal in *Lycosuchus* extends from the maxillary antrum anterior to the first postcanine along the roots of the two canines, and terminates lateral to the level of the root of the fourth incisor. Accordingly, both the canals for the alveolar rami and the canal just anterior to the external nasal rami are directed toward the canines. The morphology of the ventral ramifications of the maxillary canal is similar to that of *Olivierosuchus*, in which all three alveolar rami appear to be oriented toward the canine, but *Lycosuchus* lacks the canal for the rostral alveolar ramus just anterior to the medial and caudal alveolar rami, and the canals just anterior to the external nasal rami are here interpreted as the ones for the superior labial rami (Benoit et al., 2016a, 2018). Accordingly, the homologies of the alveolar rami do not seem to be as clear-cut as reported by (Benoit et al., 2019) in cynodonts, as they did not consider therocephalians or other therapsid outgroups in their analysis, and there is extensive variation and homoplasy in maxillary canal in general. Denser sampling of maxillary canal morphology in basal cynodonts, therocephalians and gorgonopsians is needed to see whether this variation is consistent and possibly autapomorphic for lower-level clades within these groups.

Variation in Bony Labyrinth Morphology in Therapsids

The inner ear of *Lycosuchus* generally shows the primitive condition visible in non-cynodont therapsids. As in several other non-cynodont therapsids (e.g., Castanhinha et al., 2013; Laaß, 2016; Benoit et al., 2017b), the fenestra vestibuli is positioned at the ventrolateral part of the vestibule, which is exclusively bordered by the opisthotic in *Lycosuchus*. This situation is different from what has been described for basal cynodonts such as *Galesaurus* and *Thrinaxodon*, in which the laterally facing fenestra vestibuli is located further dorsally and bordered by the opisthotic, prootic, basioccipital, and also partly by the basisphenoid wing (Fourie, 1974; Luo, 2001; Benoit et al., 2017b; Pusch et al., 2019). However, as in these and

other basal cynodonts (e.g., Fourie, 1974; Luo, 2001; Kielan-Jaworowska et al., 2004; Benoit et al., 2017b; Pusch et al., 2019), a small, globular cochlear recess is ventrally differentiated from the main part of the vestibule. Outside of Cynodontia, a cochlear recess is also present in the anomodonts *Niassodon mfumukasi* (Castanhinha et al., 2013) and *Pristerodon mackayi* (Laaß, 2016), the biarmosuchian *Lemurosaurus pricei,* and the specialized baurioid *Microgomphodon oligocynus* (Benoit et al., 2017b). The latter taxon is the only therocephalian so far for which a distinct cochlear recess has been described. However, given the limited sampling in this clade, it is currently uncertain whether the absence of a cochlear recess is typical of therocephalians. The conclusion of Benoit et al. (2017b) that a distinct cochlear recess likely evolved multiple times among therapsids requires additional sampling—it appears to be present ancestrally in therocephlians (based on the condition in *Lycosuchus*), and it is at present uncertain whether multiple origins or multiple losses of this structure characterize therapsid evolution.

Different from what is usually the case in non-mammalian therapsids and mammals, in which the anterior semicircular is the longest (e.g., Olson, 1944; Sigogneau, 1974; Luo, 2001; Kielan-Jaworowska et al., 2004; Rodrigues et al., 2013; Laaß, 2016; Araújo et al., 2017, 2018; Benoit et al., 2017b,c; Bendel et al., 2018; Pusch et al., 2019), the lateral semicircular canal appears to be the longest of the three semicircular canals in *Lycosuchus*. Several studies have shown that the elongated morphology of the semicircular canals can be linked to the animals' lifestyle (e.g., Spoor, 2003; Spoor et al., 2007; Walsh et al., 2009; Wittmer and Ridgely, 2009; Cox and Jeffery, 2010; Laaß, 2015a; Araújo et al., 2018). The anomodont *Kawingasaurus* is the only other non-mammalian therapsid described with a lateral semicircular canal larger than the anterior and posterior one, but it was suggested that its elongated morphology is related to the inflated geometry of the vestibule rather than its locomotory behavior (Laaß, 2015a). In *Lycosuchus*, the inner ear is posteriorly tilted and the curved vestibule has the typical subtriangular shape common in non-mammalian therapsids. The anterior and posterior semicircular canals are ellipsoidal, while the lateral canal is rather linear and not as curved as the other canals. This is reflected in its lower height (3.81 mm) relative to the anterior (7.21 mm) and posterior (6.20 mm) canals, but much greater width (10.88 mm) than the anterior (7.69 mm) and posterior (5.52 mm) one. In modern mammals, an elongated lateral semicircular canal is usually associated with an agile or fossorial behavior (e.g., Lindenlaub et al., 1995; Spoor et al., 2007; Cox and Jeffery, 2010; Olori, 2010). An enlarged lateral semicircular canal is also known in many aquatic non-mammalian tetrapod taxa (e.g., Benoit et al., 2013; Neenan et al., 2017; Yi and Norell, 2018; Evers et al., 2019). Based on appendicular morphology (Boonstra, 1964), *Lycosuchus* is very unlikely to represent a fossorial or aquatic animal. Nevertheless, the lengthened morphology of the lateral semicircular canal could be related to its lifestyle as an active predator, showing more adaptations for agility and cursoriality than coeval potential prey taxa (e.g., dicynodonts, dinocephalians, pareiasaurs). Other coeval therocephalians (i.e., scylacosaurids) had similar inferred

behaviors, and further sampling of bony labyrinth morphology in scylacosaurids would be useful to test whether an elongated lateral semicircular canal is related to lifestyle, or if this feature is unique to *Lycosuchus* within the clade.

Canine Replacement in Lycosuchids

The pattern of tooth replacement has long been controversial in Lycosuchidae. Originally, the family was diagnosed by the presence of two functional canines in each maxilla (Broom, 1903; Haughton and Brink, 1954; Kermack, 1956; Boonstra, 1969). However, van den Heever (1980) considered this feature to be invalid, and suggested that lycosuchids instead have one functional and one replacement canine in alternation, as in other early theriodonts. Abdala et al. (2014a) recently concurred with this interpretation and suggested a rapid rate of canine replacement in lycosuchids based on the occurrence of canine replacement in most of the specimens they investigated.

Based on our CT data for MB.R.995, we would argue that both the historical (e.g., Kermack, 1956) and more modern interpretations (e.g., van den Heever, 1980) of lycosuchid tooth replacement have merit, but hinge on the definition of what constitutes a "functional" canine. Two erupted canine crowns are definitely present in the right maxilla of MB.R.995, and both anterior and posterior would presumably be in use during prey capture. Abdala et al. (2014a: Table 6) showed that the majority of lycosuchid specimens have both the anterior and posterior canines erupted in each maxilla, in contrast to the condition in gorgonopsians and scylacosaurids in which there is usually only a single erupted canine per maxilla. In terms of positional homology, we do not think that lycosuchids are any different from gorgonopsians or scylacosaurids (i.e., they had alternating replacement of C1 in anterior and posterior alveoli, not multiple canine tooth positions homologous with those of non-therapsid sphenacodonts), but that their tooth developmental rates are different and distinctive for the family. We suggest that canine development in lycosuchids was protracted rather than rapid, such that old canines were retained for much of the development of their alternates, allowing direct replacement teeth in their own alveolus to begin forming before their loss (as visible in **Figures 12A,B**). Rather than having a worn canine fall out and be functionally replaced by its alternate, as appears to be the case in gorgonopsians and scylacosaurids, in lycosuchids both anterior and posterior maxillary canines seem to be erupted concurrently (and to some degree being functional concurrently) for much of the animal's life. In this context, it is worth noting that *Gorynychus*, recently recovered as a possible lycosuchid (Liu and Abdala, 2019), has only a single erupted canine in each maxilla and appears to show the typical scylacosaurid pattern of replacement (Kammerer and Masyutin, 2018). It is also worth noting that this delay in canine replacement, if accurate, seems to be limited to the upper dentition, as only a single lower canine per side is erupted.

Evaluating the Systematic Position of *Lycosuchus*

Our CT reconstruction of MB.R.995 provides additional information relevant to evaluating the phylogenetic position of

Lycosuchus vanderrieti. Despite damage to and loss of some cranial elements, the craniodental characters visible in the scan and described herein confirm many characters used to position *Lycosuchus* as a basal taxon in the analysis of Huttenlocker (2009) (and subsequent variants of this analysis, e.g., Huttenlocker and Sidor, 2016; Huttenlocker and Smith, 2017). These characters include, e.g., a long septomaxilla that is well-exposed on the facial surface, a high dorsal lamina of the maxilla, the presence of large upper and lower canines, and the absence of palatal processes of the maxilla and a crista choanalis. The paired vomer of MB.R.995 also demonstrates the primitive condition, based on the deeply vaulted and expanded morphology of the anterior process at its contact with the premaxilla and the absence of a ventromedian crest between the palatines.

In addition, MB.R.995 provides further information on the presence of cranial features that have previously been questioned for *Lycosuchus*, such as the presence of a vomerine process of the premaxilla (van den Heever, 1987, 1994; Huttenlocker, 2009). In the most recent phylogenetic analysis by Huttenlocker and Smith (2017), this character is listed to be present in *Lycosuchus*, in which there is a short contact between the vomerine process of the premaxilla and the anterior part of the vomer. We agree with this interpretation based on our description of this feature in MB.R.995. The presence of a lateral process of the prootic and the structure and orientation of the dorsal surface of the paroccipital process of the opisthotic have also been questioned in previous analyses (e.g., Huttenlocker, 2009; Huttenlocker and Sidor, 2016; Huttenlocker and Smith, 2017). In MB.R.995 we are able to recognize a lateral process of the prootic, but it is differently angled than in scylacosaurids and eutherocephalians, in which the lateral process of the prootic participates in the formation of the pterygoparoccipital foramen, which is absent in *Lycosuchus* (e.g., van den Heever, 1987, 1994; Huttenlocker et al., 2011; Huttenlocker and Abdala, 2015; Huttenlocker and Sidor, 2016). Despite damage, we suggest that the dorsal surface of the paroccipital process of the opisthotic was relatively straight. This character is shared with *Glanosuchus* and *Pristerognathus* to the exclusion of eutherocephalians, in which the dorsal surface of the paroccipital process of the opisthotic is deeply hollowed in the floor of the posttemporal fenestra (Huttenlocker, 2009; Huttenlocker and Sidor, 2016; Huttenlocker and Smith, 2017). Also similar to *Glanosuchus* and *Pristerognathus*, the orientation of the paroccipital process is transverse relative to horizontal in *Lycosuchus*. But this character is also present in eutherocephalians (Huttenlocker, 2009; Huttenlocker and Sidor, 2016; Huttenlocker and Smith, 2017).

The 3D reconstruction of MB.R.995 also provides new information on several internal cranial characters that have rarely been described for therocephalians and largely ignored in phylogenetic analyses of non-mammalian therapsids in general. Absence of a naso-lacrimal contact on the external snout surface is a key synapomorphy of Therocephalia (Huttenlocker, 2009), present in all known therocephalians (e.g., van den Heever, 1987, 1994; Sigurdsen, 2006; Huttenlocker et al., 2011; Huttenlocker and Abdala, 2015; Huttenlocker and Sidor, 2016; Huttenlocker and Smith, 2017; Kammerer and Masyutin, 2018) except lycideopids (Sigurdsen et al., 2012). On the internal snout

surface, however, basal therocephalians such as *Lycosuchus* and *Glanosuchus* (van den Heever, 1987, 1994; Hillenius, 1994) and akidnognathids (Sigurdsen, 2006; Sigurdsen et al., 2012) have a lacrimal bearing an anterior process that contacts the nasal. Similar to other therocephalians (van den Heever, 1987, 1994; Sigurdsen, 2006; Liu and Abdala, 2017), the dorsal surface of the posterior part of the vomer in *Lycosuchus* is characterized by a median ridge, which continues along the anterior portion of the pterygoid. In addition to the median ridge, the dorsal surface of the posterior portion of the vomer in *Lycosuchus* is characterized by two weakly-developed, transversely oriented ridges running parallel to the median one. The median ridge on the dorsal surface of the posterior part of the vomer and the ridges on the ventral surface of the nasals likely served as attachment points for cartilaginous nasal turbinals, and correspond to those described for therocephalians and several other therapsids (e.g., Fourie, 1974; van den Heever, 1987, 1994; Hillenius, 1994; Crompton et al., 2015, 2017; Bendel et al., 2018; Pusch et al., 2019). As in akidnognathids (Sigurdsen, 2006), no ridges for cartilaginous maxilloturbinals are observed in *Lycosuchus*, suggesting that they might have first evolved within cynodonts.

CONCLUSION

Our redescription of *Lycosuchus vanderrieti* based on a computed tomographic reconstruction of the skull of the specimen MB.R.995 provides new insights into the internal cranial morphology of this taxon. Most of the craniodental characters described herein support previous reports based on external characters that *Lycosuchus* represents the most basal taxon in therocephalian phylogeny. The maxillary canal and inner ear are newly described anatomical features of *Lycosuchus*, and their morphologies support the idea of extensive homoplasy in these structures, with a combination of apparent primitive and derived features among therocephalians. The maxillary canal is highly ramified (interpreted as a primitive character), and the maxillary antrum is relatively small compared to eutherocephalians. For the inner ear, notable is the presence of seemingly derived features such as a cochlear recess and the lengthened morphology of the lateral semicircular canal. A cochlear recess is otherwise only known in the Triassic

baurioid *Microgomphodon* among therocephalians, but more thorough sampling of this character in the clade is needed, while the lengthened morphology of the lateral semicircular canal could be a taxonomically-variable feature related to lifestyle. The pattern of tooth replacement in lycosuchids follows the standard pattern described in theriodonts, but teeth were likely replaced more slowly in contrast to scylacosaurids, resulting in the unusual condition of multiple erupted canines in each maxilla at most times.

DATA AVAILABILITY STATEMENT

The raw CT data supporting the conclusions of this manuscript are available in the Data Repository of the Museum für Naturkunde Berlin, https://doi.org/10.7479/hwt8-c010.

AUTHOR CONTRIBUTIONS

LP analyzed, interpreted and drafted the manuscript, and prepared all figures. JP contributed to the analysis and interpretation of the manuscript. CK was involved in the data acquisition, contributed to conceptualization, analysis and interpretation, and critical revision of the manuscript. JF was involved in the data acquisition and contributed to the conceptualization and critical revision of manuscript.

REFERENCES

Abdala, F. (2007). Redescription of *Platycraniellus elegans* (Therapsida, Cynodontia) from the Lower Triassic of South Africa, and the cladistic relationships of eutheriodonts. *Palaeontology* 50, 591–618. doi: 10.1111/j.1475-4983.2007.00646.x

Abdala, F., Jashashvili, T., Rubidge, B. S., and van den Heever, J. (2014b). "New material of *Microgomphodon oligocynus* (Eutherapsida, Therocephalia) and the taxonomy of southern African Bauriidae," in *Early Evolutionary History of the Synapsida*, eds C. F. Kammerer, K. D. Angielczyk, and J. Fröbisch (Dordrecht: Springer), 209–231.

Abdala, F., Kammerer, C. F., Day, M. O., Jirah, S., and Rubidge, B. S. (2014a). Adult morphology of the therocephalian *Simorhinella baini* from the middle Permian of South Africa and the taxonomy, paleobiogeography,

and temporal distribution of the *Lycosuchidae. J. Paleontol.* 88, 1139–1153. doi: 10.1666/13-186

Abdala, F., Rubidge, B., and van den Heever, J. (2008). The oldest therocephalians (Therapsida, Eutheriodonta) and the early diversification of *Therapsida. Palaeontology* 51, 1011–1024. doi: 10.1111/j.1475-4983.2008.00784.x

Ahlberg, P., and Clack, J. A. (1998). Lower jaws, lower tetrapods – a review based on the Devonian genus *Acanthostega. Earth Environ. Sci. Trans. R. Soc.* 89, 11–46. doi: 10.1017/S0263593300002340

Araújo, R. M., Fernandez, V., Polcyn, M. J., Fröbisch, J., and Martins, R. M. S. (2017). Aspects of gorgonopsian paleobiology and evolution: insights from the basicranium, occiput, osseous labyrinth, vasculature, and neuroanatomy. *PeerJ* 5:e3119. doi: 10.7717/peerj.3119

Araújo, R. M., Fernandez, V., Rabbitt, R. D., Ekdale, E. G., Antunes, M. T., Castanhinha, R., et al. (2018). Endothiodon cf. bathystoma

(Synapsida: Dicynodontia) bony labyrinth anatomy, variation and body mass estimates. *PLoS ONE* 13:e0189883. doi: 10.1371/journal.pone.0189883

Bendel, E.-M., Kammerer, C. F., Kardjilov, N., Fernandez, V., and Fröbisch, J. (2018). Cranial anatomy of the gorgonopsian *Cyniops robustus* based on CT-reconstruction. *PLoS ONE* 13:e0207367. doi: 10.1371/journal.pone.0207367

Benoit, J., Adnet, S., El Mabrouk, E., Khayati, H., Ben Haj Ali, M., Marivaux, L., et al. (2013). Cranial remain from Tunisia provides new clues for the origin and evolution of Sirenia (Mammalia, Afrotheria) in Africa. *PLoS ONE* 8:e54307. doi: 10.1371/journal.pone.0054307

Benoit, J., Angielczyk, K. D., Miyamae, J. A., Manger, P., Fernandez, V., and Rubidge, B. (2018). Evolution of facial innervation in anomodont therapsids (Synapsida): insights from X-ray computerized microtomography. *J. Morphol.* 279, 673–701. doi: 10.1002/jmor.20804

Benoit, J., Manger, P. R., Fernandez, V., and Rubidge, B. S. (2016b). Cranial bosses of *Choerosaurus dejageri* (Therapsida, Therocephalia): earliest evidence of cranial display structures in eutheriodonts. *PLoS ONE* 11:e0161457. doi: 10.1371/journal.pone.0161457

Benoit, J., Manger, P. R., Fernandez, V., and Rubidge, B. S. (2017b). The bony labyrinth of the late Permian Biarmosuchia: palaeobiology and diversity in non-mammalian *Therapsida*. *Palaeontology* 52, 58–77. Available online at: http://wiredspace.wits.ac.za/handle/10539/23023

Benoit, J., Manger, P. R., Norton, L., Fernandez, V., and Rubidge, B. S. (2017c). Synchrotron scanning reveals the paleoneurology of the head-butting *Moschops capensis* (Therapsida, Dinocephalia). *PeerJ* 5:e3496. doi: 10.7717/peerj.3496

Benoit, J., Manger, P. R., and Rubidge, B. S. (2016a). Palaeoneurological clues to the evolution of defining mammalian soft tissue traits. *Sci. Rep.* 6:25604. doi: 10.1038/srep25604

Benoit, J., Norton, L. A., Manger, P. R., and Rubidge, B. S. (2017a). Reappraisal of the envenoming capacity of *Euchambersia mirabilis* (Therapsida, Therocephalia) using µCT-scanning techniques. *PLoS ONE* 12:e0172047. doi: 10.1371/journal.pone.0172047

Benoit, J., Ruf, I., Miyamae, J. A., Fernandez, V., Rodrigues, P. G., Rubidge, B. S., et al. (2019). The evolution of the maxillary canal in probainognathia (Cynodontia, Synapsida): reassessment of the homology of the infraorbital foramen in mammalian ancestors. *J. Mamm. Evol.* 1–20. doi: 10.1007/s10914-019-09467-8

Boonstra, L. D. (1964). The girdles and limbs of the pristerognathid *Therocephalia*. *Ann. S. Afr. Mus.* 48, 121–165.

Boonstra, L. D. (1969). The fauna of the *Tapinocephalus* Zone (Beaufort beds of the Karoo). *Ann. S. Afr. Mus.* 56, 1–73.

Botha, J., Abdala, F., and Smith, R. M. H. (2007). The oldest cynodont: new clues on the origin and diversification of the *Cynodontia*. *Zool. J. Linn. Soc.* 149, 477–492. doi: 10.1111/j.1096-3642.2007.00268.x

Broom, R. (1903). On an almost perfect skull of a new primitive theriodont (*Lycosuchus vanderrieti*). *Trans. S. Afr. Phil. Soc.* 14, 197–205. doi: 10.1080/21560382.1903.9526025

Castanhinha, R., Araújo, R., Júnior, L. C., Angielczyk, K. D., Martins, G. G., Martins, R. M. S., et al. (2013). Bringing dicynodonts back to life: paleobiology and anatomy of a new emydopoid genus from the Upper Permian of Mozambique. *PLoS ONE* 8:e80974. doi: 10.1371/journal.pone.0080974

Cox, P. G., and Jeffery, N. (2010). Semicircular canals and agility: the influence of size and shape measures. *J. Anat.* 216, 37–47. doi: 10.1111/j.1469-7580.2009.01172.x

Crompton, A. W., Musinsky, C., and Owerkowicz, T. (2015). "Evolution of the mammalian nose," in *Great Transformations in Vertebrate Evolution*, eds K. Dial, N. Shubin, and E. Brainerd (Chicago, IL: Chicago Press), 189–203.

Crompton, A. W., Owerkowicz, T., Bhullar, B.-A. S., and Musinsky, C. (2017). Structure of the nasal region of non- mammalian cynodonts and mammaliaforms: speculations on the evolution of mammalian edothermy. *J. Vertebr. Paleontol.* 37:e1269116. doi: 10.1080/02724634.2017.1269116

Evers, S., Neenan, J., Ferreira, G. S., Werneburg, I., Barrett, P. M., and Benson, R. B. J. (2019). Neurovascular anatomy of the protostegid turtle *Rhinochelys pulchriceps* and comparisons of membranous and endosseous labyrinth shape in an extant turtle. *Zool. J. Linn. Soc.* 187, 800–828. doi: 10.1093/zoolinnean/zlz063

Fourie, S. (1974). The cranial morphology of *Thrinaxodon liorhinus* Seeley. *Ann. S. Afr. Mus.* 65, 337–400.

Haughton, A. A., and Brink, S. (1954). A bibliographical list of Reptilia from the Karoo beds of Africa. *Paleontology* 2, 1–187.

Hillenius, W. J. (1994). Turbinates in therapsids: evidence for Late Permian origins of mammalian endothermy. *Evolution* 48, 207–229.

Hillenius, W. J. (2000). Septomaxilla of nonmammalian synapsids: soft-tissue correlates and a new functional interpretation. *J. Morphol.* 245, 29–50.

Hopson, J. A. (1991). "Systematics on the nonmammalian synapsida and implications for patterns of evolution in synapsids," in *Origins of the Higher Groups of Tetrapods: Controversy and Consensus*, eds H. P. Schultze and L. Trueb (Ithaca: Comstock Publishing Associates), 635–693.

Hopson, J. A., and Barghusen, H. (1986). "An analysis of therapsid relationships," in *The Ecology and Biology of the Mammal-Like Reptiles*, eds N. Hotton, P. D. Maclean, J. J. Roth, and E. C. Roth (Washington, DC: Smithsonian Institution Press), 83–106.

Hopson, J. A., and Kitching, J. W. (2001). A probainognathian cynodont from South Africa and the phylogeny of nonmammalian cynodonts. *Bull. Mus. Comp. Zool.* 156, 5–35.

Huttenlocker, A. (2009). An investigation into the cladistic relationships and monophyly of therocephalian therapsids (Amniota: Synapsida). *Zool. J. Linn. Soc.* 157, 865–891. doi: 10.1111/j.1096-3642.2009.00538.x

Huttenlocker, A. K. (2014). Body size reductions in nonmammalian eutheriodont therapsid (Synapsida) during the end-Permian mass extinction. *PLoS ONE* 9:e87553. doi: 10.1371/journal.pone.0087553

Huttenlocker, A. K., and Abdala, F. (2015). Revision of the first therocephalian, *Theriognathus* Owen (Therapsida: Whaitsiidae), and implications for cranial ontogeny and allometry in nonmammaliaform eutheriodonts. *J. Paleontol.* 89, 645–664. doi: 10.1017/jpa.2015.32

Huttenlocker, A. K., and Sidor, C. A. (2016). The first karenitid (Therapsida, Therocephalia) from the upper Permian of Gondwana and the biogeography of Permo-Triassic therocephalians. *J. Vertebr. Paleontol.* 36:e1111897. doi: 10.1080/02724634.2016.1111897

Huttenlocker, A. K., Sidor, C. A., and Smith, R. M. H. (2011). A new specimen of *Promoschorhynchus* (Therapsida: Therocephalia: Akidnognathidae) from the Lower Triassic of South Africa and its implications for theriodont survivorship across the Permo-Triassic boundary. *J. Vertebr. Paleontol.* 31, 405–421. doi: 10.1080/02724634.2011.546720

Huttenlocker, A. K., and Smith, R. M. H. (2017). New whaitsioids (Therapsida: Therocephalia) from the Teekloof Formation of South Africa and therocephalian diversity during the end-Guadalupian extinction. *Peer J* 5:e3868. doi: 10.7717/peerj.3868

Janensch, W. (1952). Über den Unterkiefer der Therapsiden. *Paläont. Z.* 26, 229–247.

Kammerer, C. F. (2017). Anatomy and relationships of the South African gorgonopsian *Arctops* (Therapsida, Theriodontia). *Pap Paleontol.* 3, 583–611. doi: 10.1002/spp2.1094

Kammerer, C. F., and Masyutin, V. (2018). A new therocephalian (*Gorynychus masyutinae* gen. et. Sp. nov) from the Permian Kotelnich locality, Kirov Region, Russia. *PeerJ* 6:e4933. doi: 10.7717/peerj.4933

Kemp, T. S. (1979). The primitive cynodont *Procynosuchus*: functional anatomy of the skull and relationships. *Philos. Trans. Royal Soc. B* 285, 73–122. doi: 10.1098/rstb.1979.0001

Kermack, K. (1956). Tooth replacement in mammal-like reptiles of the suborders Gorgonopsia and Therocephalia. *Philos. Trans. Royal Soc.* 240, 95–133. doi: 10.1098/rstb.1956.0013

Kielan-Jaworowska, Z., Cifelli, R. L., and Luo, Z.-X. (2004). *Mammals From the Age of Dinosaurs: Origin, Evolution, and Structure*. New York, NY: Columbia University Press.

Laaß, M. (2015a). Bone-conduction hearing and seismic sensitivity of the late Permian anomodont *Kawingasaurus fossilis*. *J. Morphol.* 276, 121–143. doi: 10.1002/jmor.20325

Laaß, M. (2015b). Virtual reconstruction and description of the cranial endocast of *Pristerodon mackayi* (Therapsida, Anomodontia). *J. Morphol.* 276, 1089–1099. doi: 10.1002/jmor.20397

Laaß, M. (2016). The origins of the cochlea and impedance matching hearing in synapsids. *Acta Palaeontol. Pol.* 61, 267–280. doi: 10.4202/app.001 40.2014

Lindenlaub, T., Burda, H., and Nevo, E. (1995). Convergent evolution of the vestibular organ in the subterranean mole-rats, *Cryptomys* and *Spalax*, as

compared with the aboveground rat, *Rattus. J. Morphol.* 224, 303–311. doi: 10.1002/jmor.1052240305

Liu, J., and Abdala, F. (2017). The tetrapod fauna of the upper Permian naobaogou formation of China: 1. *Shiguaignathus wangi* gen. et sp. nov., the first akidnognathid therocephalian from China. *Peer J* 5:e4150. doi: 10.7717/peerj.4150

Liu, J., and Abdala, F. (2019). The tetrapod fauna of the upper Permian Naobaogou Formation of China: 3. *Jiufengia jiaj* gen. et sp. nov., a large akidnognathid therocephalian. *PeerJ* 7:e6463. doi: 10.7717/peerj.6463

Luo, Z.-X. (2001). The inner ear and its bony housing in tritylodontids and implications for evolution of the mammalian ear. *Bull. Mus. Comp. Zool.* 156, 81–97.

Luo, Z.-X., Crompton, A. W., and Lucas, S. G. (1995). Evolutionary origins of the mammalian promontorium and cochlea. *J. Vertebr. Paleontol.* 15, 113–121. doi: 10.1080/02724634.1995.10011211

Neenan, J. M., Reich, T., Evers, S. W., Druckenmiller, P. S., Voeten, D. F. A. E., Choiniere, J. N., et al. (2017). Evolution of the sauropterygian labyrinth with increasingly pelagic lifestyle. *Curr. Biol.* 27, 3852–3858. doi: 10.1016/j.cub.2017.10.069

Olori, J. C. (2010). Digital endocasts of the cranial cavity and osseous labyrinth of the burrowing snake *Uropeltis woodmasoni* (Alethinophidia: Uropeltidae). *Copeia* 2010, 14–26. doi: 10.1643/CH-09-082

Olson, E. C. (1944). Origin of mammals based upon cranial morphology of the therapsid suborders. *Geol. Soc. Am. Spec. Pap.* 55, 1–130. doi: 10.1130/SPE55-p1

Pavanatto, A. E. B., Kerber, L., and Dias-da-Silva, S. (2019). Virtual reconstruction of cranial endocasts of traversodontid cynodonts (Eucynodotia: Gomphodontia) from the upper Triassic of Southern Brazil. *J. Morphol.* 280, 1267–1281. doi: 10.1002/jmor.21029

Pusch, L. C., Kammerer, C. F., and Fröbisch, J. (2019). Cranial anatomy of the early cynodont *Galesaurus planiceps* and the origin of mammalian endocranial characters. *J. Anat.* 234, 592–621. doi: 10.1111/joa.12958

Rodrigues, P. G., Ruf, I., and Schultz, C. L. (2014). Study of a digital cranial endocast of the nonmammaliaform cynodont *Brasilitherium riograndensis* (Later Triassic, Brazil) and its relevance to the evolution of the mammalian brain. *Paläont. Z* 88, 329–352. doi: 10.1007/s12542-013-0200-6

Rodrigues, P. G., Ruf,.I., and Schultz, C. L. (2013). Digital reconstruction of the otic region and inner ear of the non-mammalian cynodont *Brasilitherium riograndensis* (Late Triassic, Brazil) and its relevance to the evolution of the mammalian ear. *J. Mamm. Evol.* 20, 291–307. doi: 10.1007/s10914-012-9221-2

Rowe, T., Carlson, W., and Bottorff, W. (1993). *Thrinaxodon: Digital Atlas of the Skull (CD-ROM)*. Austin, TX: University of Texas Press.

Sigogneau, D. (1974). The inner ear of *Gorgonops* (Reptilia, Therapsida, Gorgonopsia). *Ann. S. Afr. Mus.* 64, 53–69.

Sigurdsen, T. (2006). New features of the snout and orbit of a therocephalian therapsid from South Africa. *Acta Palaeontol. Pol.* 51, 63–75.

Sigurdsen, T., Huttenlocker, A. K., Modesto, S. P., Rowe, T. B., and Damiani, R. (2012). Reassessment of the morphology and paleobiology of the therocephalian *Tetracynodon darti* (Therapsida), and the phylogenetic relationships of Baurioidea. *J. Vertebr. Paleontol.* 32, 1113–1134. doi: 10.1080/02724634.2012.688693

Smith, R. M. H., Rubidge, B. S., and van der Walt, M. (2012). "Therapsid biodiversity patterns and palaeoenvironments of the Karoo Basin, South Africa," in *Forerunners of Mammals. Radiation, Histology, Biology*, ed A. Chinsamy-Turan (Bloomington, IN: Indiana University Press), 31–62.

Spoor, F. (2003). The semicircular canal system and locomotor behaviour, with special reference to hominin evolution. *Courier Forschungsinstitut Senckenberg* 243, 93–104.

Spoor, F., Garland, T., Krovitz, G., Ryan, T. M., Silcox, M. T., and Walker, A. (2007). The primate semicircular canal system and locomotion. *PNAS* 104, 10808–10812. doi: 10.1073/pnas.0704250104

Suchkova, Y. A., and Golubev, V. K. (2019). A new primitive therocephalian (Theromorpha) from the middle Permian of Eastern Europe. *Paleontol. J.* 53, 305–314. doi: 10.1134/S0031030119030158

van den Heever, J. A. (1980). On the validity of the therocephalian family Lycosuchidae (Reptilia, Therapsida. *Ann. S. Afr. Mus.* 81, 111–125.

van den Heever, J. A. (1987). *The comparative and functional cranial morphology of the early Therocephalia (Amniota: Therapsida)* [Unpublished dissertation]. University of Stellenbosch, Stellenbosch, South Africa.

van den Heever, J. A. (1994). The cranial anatomy of the early Therocephalia (Amniota: Therapsida). *Ann. Univ. Stellenbosch* 1, 1–59.

van den Heever, J. A., and Hopson, J. A. (1982). The systematic position of "Therocephalia B" (Reptilia, Therapsida). *S. Afr. J. Sci.* 78, 424–425.

Walsh, S. A., Barrett, P. M., Milner, A. C., Manley, G., and Witmer, L. M. (2009). Inner ear anatomy is a proxy for deducing auditory capability and behaviour in reptiles and birds. *Proc. R. Soc. Lond. B Biol.* 276, 1355–1360. doi: 10.1098/rspb.2008.1390

Wittmer, L. M., and Ridgely, R. C. (2009). New insights into the brain, braincase, and ear region of tyrannosaurs (Dinosauria, Theropoda), with implications for sensory organization and behavior. *Anat. Rec.* 292, 1266–1296. doi: 10.1002/ar.20983

Yi, H., and Norell, N. (2018). The bony labyrinth of *Platecarpus* (Squamata: Mosasauria) and aquatic adaptations in squamate reptiles. *Paleoworld*. doi: 10.1016/j.palwor.2018.12.001